

SPECTROSCOPIC EVIDENCE FOR THE OCCURRENCE OF NITRATES IN LIGNITES

Clarence Karr, Jr., Patricia A. Estep, and John J. Kovach

Morgantown Coal Research Center, Bureau of Mines,
U. S. Department of the Interior, Morgantown, W. Va. 26505

INTRODUCTION

As part of a broad program of coal research at the Morgantown Coal Research Center, U. S. Bureau of Mines, extensive studies are being conducted on minerals in coal using a variety of analytical techniques. A method was successfully applied for obtaining unaltered mineral matter from coal by means of an electronic low-temperature asher (1). Significant amounts of sodium and alkaline earth nitrates were identified in lignite ashes obtained by this technique. Nitrates have not been found, however, in the ashes from any of the bituminous or anthracite coals examined to date; nitrates appear to predominate only in the ashes of lignites from the Fort Union Formation of the Great Plains coal area. These findings raised the question as to whether nitrates are formed by chemical reaction in the oxygen plasma of the asher, or are original mineral constituents of the coals. It was therefore desirable to determine, through independent methods, if nitrates are present in lignite.

This paper describes the water extraction of inorganic nitrates and their identification in the extracts by infrared spectroscopy. The presence of nitrates as original mineral constituents was confirmed, but the amount of nitrate that may have been chemically produced in the asher was not determined. The amounts of nitrates in these lignites were estimated from x-ray powder patterns of the untreated whole coals. Oxalates and sulfates were also identified by infrared spectroscopy in the water-soluble material.

EXPERIMENTAL

Coal samples were preground for 30 min. in a tungsten carbide ball mill (Spex)* and dried at 105° C for 4 hr. under a 300 ml/min. stream of nitrogen. When the moisture content is high (over about 20 pct), the coal must be predried for efficient grinding.

Infrared Spectroscopy

Pellets were prepared for infrared analysis by blending 1 mg of the sample with 500 mg of cesium iodide powder and preparing the pellet by triple pressing. The resulting pellet, 0.80 mm by 13 mm, was then scanned immediately on a Perkin-Elmer 621 infrared grating spectrophotometer purged with dry air.

* Reference to specific brands is made for identification only and does not imply endorsement by the Bureau of Mines.

Low-Temperature Oxidation

A one-gram sample of preground coal was ashed in Tracerlab's Model LTA-600L low-temperature asher at 145° C. A stream of excited oxygen produced by a radio frequency electromagnetic field of 13.56 MHz, passed over the coal at 1 mm Hg pressure, and completely removed the organic matter in 70 to 90 hr. Temperature measurements were made with a Huggins Laboratories Mark I Infrascop.

Water Extraction

Stepwise water extractions were conducted on three lignites. The available analytical data on the original coals are shown in Table 1. The procedure is described as follows: A preground sample of coal of known moisture content was placed in a Whatman paper Soxhlet extraction thimble between two layers of glass wool inert filler. All equipment was prewashed with distilled-deionized water. Sufficient distilled-deionized water (200 ml) was added to completely cover the sample when the thimble was placed in a 1,000 ml beaker. The sample was covered with water at all times and the water temperature was held at 90° C for 2 hr. The water solution was then removed, filtered, and carefully evaporated to dryness on a hot plate. An infrared spectrum was then obtained on this water soluble residue. The extraction was continued in this manner for a minimum of 5 to 10 separate extractions, each with a fresh volume of water as extractant. The extractions were not exhaustive or quantitative, but rather were conducted until a relatively invariant infrared spectrum was obtained.

X-ray Diffraction

Samples were mounted in 0.5 mm glass capillaries and were analyzed with iron-filtered $\text{CoK}\alpha$ radiation, using a two radian Debye-Scherrer camera for optimum resolution. The average exposure time for coal samples was 12 hr., and the use of cobalt radiation minimized the background intensity. Both low-temperature ash samples and water extraction residues provided good patterns with exposure times of 7 to 8 hr.

RESULTS AND DISCUSSION

Water Extractions

Nitrates can be water extracted from lignite only under certain conditions, and there are apparently several factors involved in a successful extraction. Several initial extraction attempts failed. For example, an extraction was attempted on the Beulah, N. D., lignite as received, with no pregrinding, and very little nitrate was extracted. Another sample of the same coal was then preground in a tungsten carbide ball mill and the identical extraction procedure repeated. Successful extraction of nitrates was then achieved and, in addition, the total material extracted was increased. Thus it became apparent that the particle size of the coal plays an important role in the nitrate extraction. For a variation in extraction technique, a 90-hr. 90° C extraction of lignite from Minot, N. D., was subsequently made in an ordinary Soxhlet apparatus, using 3.7 grams of coal and 150 ml of water. The infrared spectrum of the extract (curve a, Figure 1) showed that it

was predominantly sodium sulfate, with only a small amount of nitrates, and qualitatively very similar to the first extract from Dawson County, Mont., lignite obtained by the described extraction in a beaker after only 2 hr. (extract 1, Figure 2). It is apparent that the extraction process is not a simple function of relative solubilities, but must be a complex interplay of the ion exchange properties of the various ions present, their concentrations, and the adsorption properties of the coal substance. The salts extracted thus represent the equilibrium conditions achieved. The complexity of the system is further emphasized by the fact that sodium sulfate was not detected in the low-temperature ash from the Minot, N. D., coal, and that nitrates are generally much more soluble in water than sulfates. Sodium sulfate could not have decomposed in the low-temperature ash, as demonstrated by the fact that it is found in boiler deposits that are formed at much higher temperatures. The phenomenon responsible for the selective tenacity that the coal has for nitrates remains unexplained. One possibility is that nitrates are encapsulated in the plant structure retained by this low-rank coal. Another possibility is that nitrates are preferentially adsorbed on clays in the coal or at active sites in the coal structure. It is not known if the discrepancy between the amounts of nitrate extracted (less than 2 wt pct of the coal) and the amounts found in the low-temperature ashes is due to the production of additional nitrate during ashing.

Infrared Analysis

It was not possible to verify the presence of nitrates from infrared spectra of the coal itself because of the high background absorption of organic material. The infrared spectra of the material from five successive extraction steps for the Montana coal are shown in Figure 2. The overall spectral characteristics show that the residues are predominantly inorganic. The weak CH stretching vibrations appearing at 2850 and 2930 cm^{-1} in all extracts are assigned to fine residual coal particles which could not be filtered. Extract I is predominantly sodium sulfate, as evidenced by the strong fundamental vibration at 1128 cm^{-1} , characteristic for the sulfate ion, and the weaker bands at 990, 628, 612, and 225 cm^{-1} , specific for sodium sulfate. The minor bands are unique and make possible a clear distinction between sodium sulfate and other probable sulfates such as calcium and magnesium sulfates. Sodium sulfate bands can be followed through successive extracts and are seen to gradually decrease. Also in the first extract there appears a weak but definite absorption band at 1360 cm^{-1} . The intensity of this band increases in each successive extract, as seen in Figure 2, until it becomes a major band in extract 5.

A careful study of many infrared spectral-structure correlations (2, 3, 4, 5, 6, 7) shows that there are few inorganic ions absorbing in this spectral region. Table 2 is a compilation of data from these references, showing the only possible assignments if one makes the regular assumption that the band at 1360 cm^{-1} is a characteristic group frequency, representing a class of ions. This assumption is well justified on the basis of the intensity of the band. From the data in this table and the infrared spectra of the extracts in Figure 2, a systematic elimination of all ions can be made with the exception of nitrates. For example, the nitrite ion can be readily eliminated on the basis that a strong asymmetric stretch (ν_3) for the N-O bond is required near 1260 cm^{-1} (7), and this cannot be observed in the

spectra of any of the extracts. Tetraborates, $(B_4O_7)^{2-}$, exhibiting very complex infrared spectra, require a strong absorption near 1000 cm^{-1} and metaborates, $(BO_2)^-$, require one near 950 cm^{-1} . Neither are observed in any of the spectra of the extracts.

With nitrate as the remaining possibility, the infrared spectra of a large number of inorganic nitrates were examined, both from the literature (8, 9, 10, 11, 12, 13) and from this laboratory. The absorption band observed in nearly all inorganic nitrates near 1360 cm^{-1} has been assigned to the asymmetric N-O stretching vibration (ν_3) of the nitrate ion. Its very narrow range for the inorganic class of nitrates (30 cm^{-1}) increases its specificity and usefulness. The nitrate interpretation is given additional strong support by the observation of a weak band at 825 cm^{-1} , the out-of-plane bending vibration (ν_2) for the nitrate ion, appearing well resolved in the fourth and fifth extracts, where the 1360 cm^{-1} band has become very intense. It is not possible, from the infrared spectra of these extracts alone, to establish with certainty the identity of the specific cation or cations accompanying the nitrate ion. Within nitrates as a class, the ν_2 vibration varies in position and can be used along with additional bands for a specific identification of the cation. Figure 3 presents the infrared spectra of sodium nitrate and calcium nitrate, demonstrating the relative simplicity of the infrared spectra for inorganic nitrates in general and shows the reduced intensities of additional bands. These weaker bands could not be observed in the water extracts, but in the low-temperature ashes, where nitrates appear more concentrated, all of these weaker bands have been observed.

The shoulder appearing at 1400 cm^{-1} , along with the 1360 cm^{-1} band in the water extracts, suggests the presence of alkaline earth nitrates. The splitting of the N-O stretching vibration (ν_3) into two bands for polyvalent metal nitrates and specifically for alkaline earth nitrates has been discussed by Vratny (9), Ferraro (11), and Buijs (12). This split, demonstrated in the spectrum of calcium nitrate in Figure 3, has been assigned to a reduction in symmetry and also to increasing covalent character of the nitrate ion. Infrared spectra of the low-temperature ashes give even stronger evidence for the presence of alkaline earth nitrates: The ν_3 split is observed, the ν_2 for calcium and magnesium nitrates is observed, and the bands due to water of hydration are more intense, as required for these nitrates. Carbonates in the water extracts are a possible assignment for the 1400 cm^{-1} band. However, the carbonate ν_2 out-of-plane bending in the 860 to 880 cm^{-1} region, comparable in intensity to the ν_2 for nitrates, was not observed in spectra of the extracts or in the low-temperature ashes.

As the extraction continues, the hemihydrate of calcium sulfate ($CaSO_4 \cdot 1/2H_2O$) gradually appears and can be positively identified in extract 5 by its characteristic bands at 650 and 592 cm^{-1} , as well as by the strong sulfate group vibration at 1147 cm^{-1} . The distinction between $CaSO_4$, $CaSO_4 \cdot 1/2H_2O$, and $CaSO_4 \cdot 2H_2O$ can be readily made in the infrared (1). The presence of calcium sulfate in the form of the hemihydrate indicates that the maximum temperature during evaporation of water from the extract lies between 128° and 163° C because of the following known conversions:



This indicates that the extract was not subjected to high temperatures and precludes oxidation. The position of calcium sulfate in the extraction after sodium sulfate is in line with the relative cation exchange power of calcium and sodium. Kaolinite, a clay mineral, appears in significant amounts in extracts 3 and 4 and is identified by its bands at 3695, 3620, 1100, 1030, 1010, 930, 910, 790, 750, 690, 530, 462, 425, 340, and 268 cm^{-1} . Its presence in these water extracts indicates a particle size too fine to be filtered. The strong, broad absorption bands at 3440 and 1613 cm^{-1} are vibrations assigned to water of crystallization.

The bands at 1330 and 777 cm^{-1} in this extraction were observed in the same relative intensities in all water extractions attempted, and were suspected of belonging to oxalates. Support for this interpretation was obtained from a methanol separation made on the water extract of the Minot, N. D., coal. The water extract (curve a, Figure 1) shows the suspected oxalate bands at 1330 and 777 cm^{-1} , with medium intensities. Curves (b) and (c) are the infrared spectra of the methanol soluble and methanol insoluble material, respectively. Consistent with the known insolubility of oxalates in alcohols, these bands are enhanced in the methanol insoluble material. The position and relative intensities of these two bands, along with newly resolved bands at 1640 and 507 cm^{-1} seen in curve (c) of Figure 1, are in good agreement with the infrared spectra of sodium and calcium oxalates. The observed frequencies of 1640, 1330, and 777 can be assigned to the carboxylate (O-C-O) vibrations of the asymmetric stretch (ν_9), the symmetric stretch (ν_{11}), and a deformation (ν_{12}), respectively (14). The higher solubilities of alkali oxalates compared to those of alkaline earth oxalates would support the presence of sodium oxalate in the water extracts, although increased solubilities are known when soluble oxalates combine with insoluble oxalates to form double salts. Also, calcium oxalate requires two additional medium bands at 660 and 305 cm^{-1} , which do not appear. If calcium oxalates were present in small amounts, it could be in the form of a fine particle suspension, similar to the occurrence of kaolinite in these water extracts. In view of the widespread occurrence of oxalates in plant matter, their identification in lignites is not at all unlikely.

The methanol separation shown in Figure 1 provides additional support for the presence of nitrates in lignite water extracts. As previously described, this 90-hr. Soxhlet extraction yielded only minor amounts of nitrate, as indicated by the weak absorption at 1360 cm^{-1} in curve (a). The enhancement of this band, seen in curve (b), shows that methanol has selectively dissolved nitrate, while the sodium sulfate at 1128, 990, 628, 612, and 225 cm^{-1} in curve (c) remains predominantly in the insoluble portion. This separation is in good accord with the known relative solubilities in methanol, and with methanol solubility studies on mixtures of sodium nitrate and sodium sulfate.

The stepwise extractions on the two North Dakota coals proceeded in a qualitatively similar fashion to that shown in Figure 2 for the Montana coal, achieving the same concentration of nitrate but with considerably higher amounts of oxalates. Atomic absorption analyses on the Minot, N. D., coal, both prior to and following the extraction, show that essentially all sodium was removable with distilled, demineralized water.

X-ray Analysis

X-ray powder patterns were obtained on water extracts and on the original coal samples in order to verify the presence of nitrates. Good peak-to-background ratios were obtained from the coal samples by using $\text{CoK}\alpha$ radiation (1.79 Å), although long exposure times (12 hr.) were required. The use of radiation with shorter wavelengths (e. g. . $\text{CuK}\alpha$. 1.54 Å) resulted in a high background, presumably because of increased Compton scattering by the organic matrix.

The interplanar spacings obtained for the Montana coal, and the ASTM data (15) for the minerals identified, are listed in Table 3. X-ray analysis of the coal samples indicated the presence of quartz, kaolinite, gypsum ($\text{CaSO}_4 \cdot 2\text{H}_2\text{O}$), and the nitrates of calcium and sodium. Several low-intensity lines from the ASTM data are not listed. Some kaolinite lines are absent presumably due to preferred orientation effects. The form of calcium sulfate generally occurring in coal is gypsum (1), and this is an important factor in the x-ray interpretation. Upon being subjected to low-temperature ashing or evaporation after water extraction, gypsum dehydrates to the hemihydrate. The x-ray spectral lines for the hemihydrate overlap the lines of sodium nitrate, precluding the positive identification of sodium nitrate in either the low-temperature ash or the water extract. Gypsum, however, with a completely different crystal structure, has a set of lines that do not seriously overlap those of sodium nitrate. In addition, both CaSO_4 and $\text{CaSO}_4 \cdot 1/2\text{H}_2\text{O}$ have specific lines that were used in determining that they were not present in the coal. As a result, the presence of sodium nitrate can be verified in the original coals, using the strong line at 3.03 Å and the weaker line at 1.463 Å. On the basis of the observed intensities of the sodium nitrate lines, its amount was estimated to be about 5 wt pct. The intensities of the x-ray lines were considerably greater than those for the minimum detectable amount, about 1 wt pct.

Several lines for calcium nitrate were present in the powder pattern of the Beulah, N. D., lignite and this supported the infrared evidence of alkaline earth nitrates in the water extract of this lignite. The presence of sodium oxalate could not be verified by x-ray of the lignites because all the strong lines of this compound were overlapped by those of other substances present. However, the absence of the unique lines for potassium and calcium oxalates and hydrates indicated that these particular oxalates were not present.

ACKNOWLEDGMENTS

Special thanks are due Edward E. Childers, Morgantown Coal Research Center, for obtaining infrared spectra and conducting the low-temperature oxidations on the coals. We also thank John J. Renton, Geology Department, West Virginia University, for x-ray data, and Edward L. Obermiller, Consolidation Coal Company, Library, Pa., for analytical data.

REFERENCES

1. Estep, Patricia A., Kovach, John J., and Karr, Clarence, Jr. Quantitative Infrared Multicomponent Determination of Minerals Occurring in Coal. *Anal. Chem.*, 1968 (Feb.), 40, 358 to 363.
2. Ferraro, John R. *Inorganic Infrared Spectroscopy*. J. Chem. Ed., 1961 (April), 38, 201 to 208.
3. Yoganarasimhan, S. R., and Rao, C. N. R. Correlation Chart for Group -1 Frequencies in Inorganic Substances for the Infrared Region 4000 - 300 cm^{-1} . *Chemist-Analyst*, 1962; 51, 21 to 23.
4. Miller, Foil A., and Wilkins, Charles H. Infrared Spectra and Characteristic Frequencies of Inorganic Ions. *Anal. Chem.*, 1952 (Aug.), 24, 1253 to 1294.
5. Colthup, N. B., Daly, L. H., and Wiberley, S. E. *Introduction to Infrared and Raman Spectroscopy*. Academic Press, Inc., New York, 1964, 511 pp.
6. Nakamoto, Kazuo. *Infrared Spectra of Inorganic and Coordination Compounds*. John Wiley & Sons, Inc., New York, 1963, 328 pp.
7. Bellamy, L. J. *The Infra-red Spectra of Complex Molecules*. John Wiley & Sons, Inc., New York, 1958, 425 pp.
8. Kalbus, Gene Edgar. *The Infrared Examination of Inorganic Materials*. University Microfilms, Inc., Ann Arbor, Michigan, 1957, 207 pp.
9. Vratny, Frederick. Infrared Spectra of Metal Nitrates. *Appl. Spectroscopy*, 1959, 13, 59 to 70.
10. Sadtler Research Laboratories, Philadelphia, Pa. *High Resolution Spectra of Inorganics and Related Compounds*. Vols. 1 and 2, 1965; vols. 3 and 4, 1967.
11. Ferraro, John R. The Nitrate Symmetry in Metallic Nitrates. *J. Molecular Spectroscopy*, 1960, 4, 99 to 105.
12. Buijs, K., and Schutte, C. J. H. The Infra-red Spectra of the Anhydrous Nitrates of Some Alkali and Alkaline Earth Metals. *Spectrochim. Acta*, 1962, 18, 307 to 313.
13. Miller, Foil A., and Carlson, Gerald L. Infrared Spectra of Inorganic Ions in the Cesium Bromide Region (700-300 cm^{-1}). *Spectrochim. Acta*, 1960, 16, 135 to 235.
14. Schmelz, M. Judith, Miyazawa, Tatsuo, Mizushima, San-ichiro, Lane, T. J., and Quagliano, J. V. Infra-red Absorption Spectra of Inorganic Coordination Complexes--IX. Infra-red Spectra of Oxalato Complexes. *Spectrochim. Acta*, 1957, 9, 51 to 58.

15. American Society for Testing and Materials, 1916 Race Street, Philadelphia, Pa. X-Ray Powder Data File, 1966, 1 to 683.

TABLE 1. Lignite analyses, percent

	R. A. Newton mine, Dawson County, Mont.	Beulah, Mercer County, N. D.	Minot, Ward County, N. D.
Nitrogen	0.61	0.56	1.13
Moisture	26.2	37.6	38.4
Low-temperature ash	24.0	12.0	9.6
High-temperature ash	19.3	6.56	5.19
High-temperature ash composition:			
Na ₂ O	6.6	8.9	13.2
CaO	11.7	20.4	34.2
MgO	3.8	7.2	7.1
K ₂ O	0.8	0.4	0.75

TABLE 2. Possible polyatomic ions absorbing at 1360 cm⁻¹*

Ion	Absorption in spectral** region of 1360 cm ⁻¹		Additional absorption bands required
	Average of range cm ⁻¹	Range cm ⁻¹	Average of range cm ⁻¹
<u>N-O Stretching Vibration</u>			
1. Nitrate, (NO ₃) ⁻	1360 (s)	30	820 (m, sharp)
2. Nitrite, (NO ₂) ⁻	1350 (w)	50	1260 (s) 800 (w)
<u>B-O Stretching Vibration</u>			
3. Tetraborate, (B ₄ O ₇) ²⁻	1400 (m-s)	110	1000 (s) 1080 (w-s)
4. Metaborate, (BO ₂) ⁻	1340 (m-s)	70	950 (s)

* Composite data from references 2 through 13.

**Intensity designations in parentheses are: s = strong, m = medium, w = weak.

TABLE 3. X-ray analysis of Dawson County, Mont., lignite

dÅ	Relative intensity*	Identification	NaNO ₃	Gypsum	Kaolinite	Quartz
7.65	M	Gypsum		7.58 ¹⁰⁰		
7.07	M	Kaolinite			7.15 ¹⁰⁰	
4.41	W	Kaolinite			4.45 ⁵⁰	
4.28	S	Gypsum, kaolinite, quartz		4.27 ⁵¹	4.35 ⁶⁰	4.26 ³⁵
4.13	W	Kaolinite			4.17 ⁶⁰ or 4.12 ³⁰	
3.83	W	NaNO ₃ , gypsum, kaolinite	3.89 ⁶	3.79 ²¹	3.84 ⁴⁰	
3.55	M	Kaolinite			3.57 ¹⁰⁰	
3.36	W	Kaolinite			3.37 ⁴⁰	
3.32	W	Quartz				3.343 ¹⁰⁰
3.26	W					
3.20	W					
3.18	W	Gypsum, kaolinite		3.163 ³	3.14 ²⁰	
3.08	M	Gypsum, kaolinite		3.059 ⁵⁷	3.09 ²⁰	
3.03	M	NaNO ₃	3.03 ¹⁰⁰			
2.97	VW					
2.85	M	NaNO ₃ , gypsum	2.81 ¹⁵	2.867 ²⁷		
2.67	M	Gypsum, kaolinite		2.679 ²⁸	2.75 ²⁰	
2.55	W	NaNO ₃ , gypsum, kaolinite	2.53 ⁹	2.591 ⁴	2.55 ⁷⁰	
2.50	W	Gypsum, kaolinite, quartz		2.495 ⁶	2.52 ⁴⁰ or 2.486 ⁸⁰	2.458 ¹²
2.32	MW	NaNO ₃ , kaolinite	2.311 ²⁴		2.374 ⁷⁰ or 2.331 ⁹⁰	

Continued

TABLE 3. X-ray analysis of Dawson County, Mont., lignite (continued)

dÅ	Relative intensity*	Identification	NaNO ₃	Gypsum	Kaolinite	Quartz
2.27	W	Kaolinite, quartz			2.284 ⁸⁰	2.282 ¹²
2.20	VW	Kaolinite, quartz			2.182 ³⁰	2.237 ⁶
2.11	W	NaNO ₃ , kaolinite, quartz	2.125 ⁹		2.127 ²⁰	2.128 ⁹
2.08	W	Gypsum		2.080 ¹⁰		
2.04	W	Gypsum, kaolinite		2.073 ⁸	2.057 ⁵	
1.98	W	NaNO ₃ , kaolinite, quartz	1.947 ⁴		1.985 ⁷⁰	1.98 ⁶
1.89	W	NaNO ₃ , gypsum, kaolinite	1.898 ¹⁶	1.898 ¹⁶	1.892 ²⁰	
1.88	W	NaNO ₃ , gypsum, kaolinite	1.880 ⁷	1.879 ¹⁰	1.865 ⁵	
1.81	W	Gypsum, kaolinite, quartz		1.812 ¹⁰	1.835 ⁴⁰	1.817 ¹⁷
1.77	W	Gypsum, kaolinite		1.778 ¹⁰	1.778 ⁶⁰	
1.66	W	NaNO ₃ , gypsum, kaolinite, quartz	1.652 ⁴	1.664 ⁴	1.682 ¹⁰	1.672 ⁷
1.61	W	NaNO ₃ , gypsum, kaolinite	1.629 ⁴	1.621 ⁶	1.616 ⁷⁰	
1.54	W	NaNO ₃ , quartz	1.544 ²			1.541 ¹⁵
1.48	W	NaNO ₃	1.463 ⁴			

* S = strong, M = medium, W = weak, V = very.

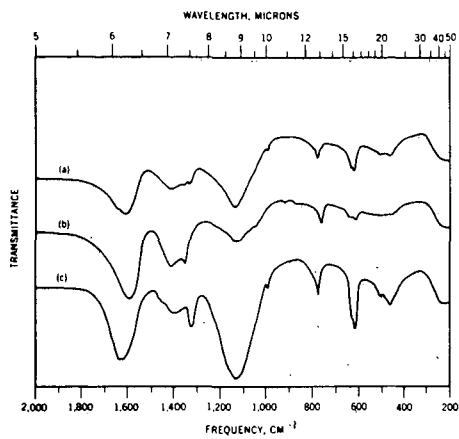


FIGURE 1. - Infrared spectra of (a) Soxhlet water extract of a North Dakota lignite; (b) methanol soluble material from (a); (c) methanol insoluble material from (a).

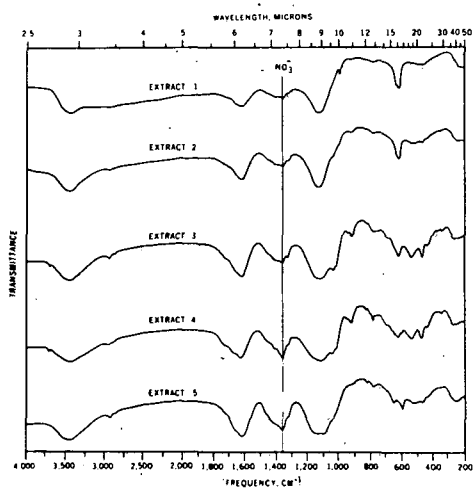


FIGURE 2. - Infrared spectra of successive water extracts from a Montana lignite.

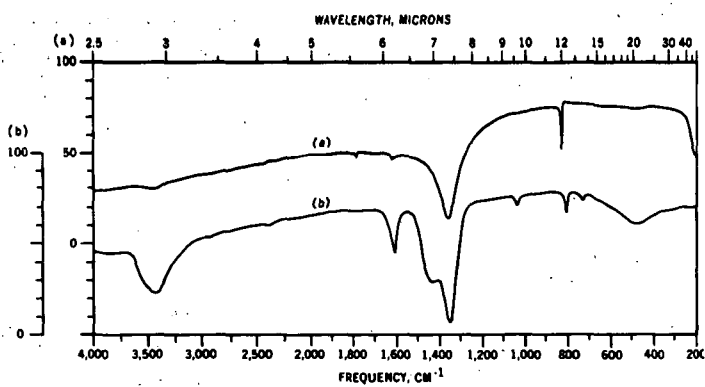


FIGURE 3. - Infrared spectra of (a) sodium nitrate, NaNO_3 ; (b) calcium nitrate, $\text{Ca}(\text{NO}_3)_2 \cdot 4\text{H}_2\text{O}$.

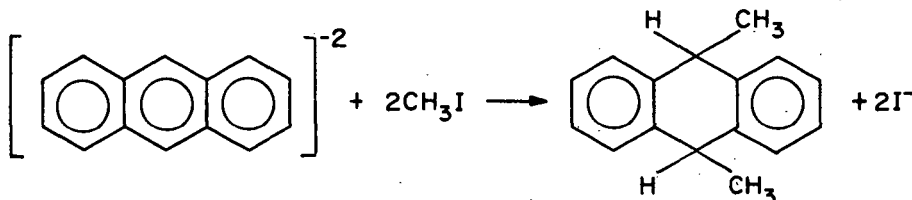
SOLVATION AND REDUCTIVE ALKYLATION OF COAL VIA A
"COAL ANION" INTERMEDIATE

Heinz W. Sternberg and Charles L. Delle Donne

Pittsburgh Coal Research Center, Bureau of Mines,
U. S. Department of the Interior,
4800 Forbes Avenue, Pittsburgh, Pennsylvania 15213

INTRODUCTION

During the last decade a large amount of work has been published on the formation, structure, and reactions of aromatic hydrocarbon anions.^{1,2} These anions are readily formed when aromatic hydrocarbons, dissolved in a suitable solvent, are treated with alkali metals. For example, naphthalene³ dissolved in tetrahydrofuran or hexamethylphosphoramide, $[(CH_3)_2N]_3PO$, reacts with one or two moles of lithium to form the green naphthalene mono-anion, $[C_{10}H_8]^-$ or the red naphthalene di-anion $[C_{10}H_8]^{2-}$ depending on the amount of lithium used. Aromatic hydrocarbon anions react with a wide variety of reagents such as alkyl halides,² carbon dioxide,⁴ acetyl chloride,⁵ aldehydes,⁶ ketones⁶ and compounds containing active hydrogen atoms such as alcohols and water.⁷ For example, anthracene di-anion reacts⁸ with methyl iodide to give among other products 9,10-dimethyl-9,10-dihydroanthracene:



Since coal is believed to contain clusters of condensed aromatic rings, we thought that it might be possible to introduce alkyl groups into the coal molecule by forming aromatic hydrocarbon anions in the coal molecule and then allowing these anions to react with alkyl halides.

EXPERIMENTAL DATA AND RESULTS

Reagents. - Metallic lithium, naphthalene, and hexamethylphosphoramide, (HMPA), were of the highest purity available commercially. Lithium and naphthalene were used as received. HMPA was purified by vacuum distillation and the fraction boiling between 89° and 92° at 4 to 5 mm were used.

Coal. - In all experiments, a hand-picked Pocahontas (lvb) vitrain sample (ground to pass 325 mesh) was used.

Solvation of Coal by Treatment with Lithium in HMPA. - Under a protective cover of nitrogen, 0.1247 gram of vitrain, 0.22 millimole (0.0152 gram) of lithium, and 15 ml of HMPA were placed in a test tube provided with a screw cap. The sealed test tube was gently tumbled (about 40 revolutions per minute) for 8 hours to provide adequate agitation. The contents of the test tube were then centrifuged. The supernatant dark-red solution was pipetted off and the residue treated with 15 ml of HMPA; the resulting suspension was centrifuged and the supernatant solution pipetted off as before. The residue was washed with water until the washings were neutral and the residue was collected on a weighed glass filter. After

drying in vacuo at 100°C, the residue weighed 0.0135 gram, corresponding to 10.8 percent of the original sample. This showed that 89.2 percent of the vitrain was solvated by treatment with lithium in HMPA. By itself, HMPA is only capable of solvating 3 percent of the vitrain.

Alkylation of Naphthalene. - A 1.005 gram sample of naphthalene (7.85 millimoles) and 150 ml of HMPA were placed in a 500 ml Erlenmeyer flask under a protective cover of nitrogen and 0.1328 gram (19.1 millimoles) of lithium wire cut into small pieces was added to the flask. The contents of the flask were stirred by means of a glass enclosed magnetic stirring bar for 8 hours, during which time the color of the solution turned first to a dark green (color of the mono-anion) and then to a dark red (color of the di-anion of naphthalene). The solution was cooled to 5°C and 2.4 ml (30 millimoles) of ethyl iodide was slowly added to the solution with stirring. The reaction mixture was poured into ice water and the aqueous mixture was extracted with pentane. The pentane extract was in turn treated with dilute acid, sodium bicarbonate solution and water to remove any HMPA, and the pentane extract was then freed of pentane. Mass spectrometric and glc analyses of the reaction product indicated that about 30 percent of the naphthalene had been converted to a mixture consisting of di- and tetra-hydro derivatives of mono- and di-methyl and ethyl naphthalene. The main product, on the basis of relative mass peak heights, consisted of equal amounts of ethyl- and diethyldihydro-naphthalene. The reaction product was again alkylated as described above. Analysis of the reaction product from this second alkylation indicated that the overall amount of naphthalene converted was 70 percent, the main product again being ethyl- and diethyldihydronaphthalene.

Alkylation of Coal. - A 1.5290-gram sample of the vitrain (ground to pass 325 mesh) and 150 ml of HMPA were placed in a 500 ml Erlenmeyer flask under a protective cover of nitrogen and 0.2073 gram (29.9 millimoles) of lithium wire was added to the contents of the flask. After the contents of the flask had been stirred for 8 hours, 3 ml (37.5 millimoles) of ethyl iodide was added as described above for the alkylation of naphthalene. The reaction mixture was poured into oxygen-free ice water. The precipitate was washed repeatedly first with water until the washings were neutral and then with ethanol to remove any trace of HMPA. The recovered material, dried in vacuo at 100°, weighed 1.6962 grams and was 35 percent soluble in benzene at room temperature. A 0.4790-gram sample of the recovered coal was again subjected to alkylation with proportional amounts of HMPA and lithium (60 ml and 0.0754 gram, respectively) as described above. The weight of the recovered material was 0.6263 gram and the benzene solubility 86 percent. Table 1 shows the ultimate analysis for the original vitrain, and for the vitrains after the first and second alkylation. Table 2 gives the benzene solubilities of the original and alkylated vitrains at room temperature. Figure 1 shows the infrared spectrum (KBr-pellet) of the original vitrain, that of the vitrain subjected to one and that of the vitrain subjected to two alkylations.

TABLE 1. - Ultimate analysis¹ of alkylated Pocahontas #3 vitrain

	C	H	N	S	O ²	P	I	Ash
Original vitrain	84.85	4.35	1.14	0.63	3.40	0.00	0.00	5.63
First alkylation	82.99	5.92	1.43	.53	4.22	.01	.84	4.06
Second alkylation	81.94	6.69	1.64	.47	3.06	.26	.00	5.94

¹ Dry basis.

² By difference.

TABLE 2. Benzene solubility of original and alkylated Pocahontas vitrain

<u>Vitrains</u>	<u>Percent soluble</u>
Original vitrain	0.5
First alkylation	35.2
Second alkylation	85.8

DISCUSSION

Solvation of Coal, Formation of "Coal Anion"

Although only 3 percent soluble in HMPA, coal becomes almost 90 percent soluble on addition of lithium to a suspension of coal in HMPA. This tremendous increase in solubility on addition of lithium is almost certainly due to the formation of aromatic anions of large volume produced by the transfer of electrons to the coal molecule according to



These negatively charged aromatic clusters probably repel each other and are readily solvated because their charges are distributed over a large volume. The lithium cation on the other hand is effectively solvated by HMPA. Whatever the explanation, the high solubility of the "coal anion" offers an opportunity to introduce alkyl groups into the coal molecule.

Alkylation of Naphthalene

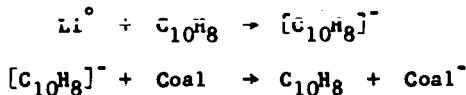
Before attempting to alkylate coal via the "coal anion" in HMPA we explored the feasibility of alkylating a model compound, i.e., naphthalene in this solvent. Treatment of naphthalene with lithium in HMPA produced the dianion $[\text{C}_{10}\text{H}_8]^{-2}$, but alkylation of the di-anion with ethyl iodide yielded in addition to the expected ethyl derivatives also small amounts of methyl derivatives of naphthalene, di- and tetrahydronaphthalene. Apparently, HMPA acted to some extent as a methylating agent under the conditions of our experiment.

Alkylation of Coal

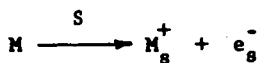
Alkylation of coal with ethyl iodide, carried out by the same procedure as the alkylation of naphthalene, yielded an ethylated coal, which was 35 percent soluble in benzene at room temperature and whose infrared spectrum (KBr-pellet) showed distinct bands (Figure 1) attributable to a methyl group (7.25 μ) and its associated stretching vibration (3.4 μ). A second alkylation of the recovered coal yielded a product which was now 85 percent soluble in benzene and whose IR spectrum (Figure 1) shows bands of increased intensity at 3.4 μ and 7.25 μ . A rough estimate of the amount of ethyl groups introduced into the coal may be obtained by assuming that the increase in weight of the recovered material over the starting coal after alkylation is due to the addition of ethyl groups. On the basis of this assumption the amount of ethyl groups introduced into the coal molecule after two alkylations corresponds to about one methyl group per 5 carbon atoms. Some methylation in addition to ethylation of the coal may have taken place in analogy to the reductive ethylation of naphthalene in HMPA described in the experimental part.

Alkylation of Coal in Tetrahydrofuran

Alkylation of coal is not restricted to the use of HMPA. For example, exploratory experiments have shown that coal can be readily alkylated in tetrahydrofuran provided a small amount of naphthalene is added which functions as an electron transfer agent



in the formation of the coal anion. In the case of HMPA, an electron transfer agent is not required since alkali metals readily dissolve in HMPA with formation of solvated cations and solvated electrons according to



where S stands for the solvent, HMPA.^{9,10}

Structure of Coal and of Petroleum Asphaltenes

The fact that introduction of alkyl groups into the coal structure produces a benzene soluble material points to a relationship between alkylated coal and petroleum asphaltenes. The latter are soluble in benzene in spite of the fact that they contain a larger number of rings^{11,12} (8 to 9) per cluster than coal¹² (3 to 4 rings per cluster). However, petroleum asphaltenes, in contrast to coal, contain a considerable number of alkyl groups attached to the aromatic clusters.¹¹ The fact that the introduction of alkyl groups into coal converts coal into a benzene soluble product indicates that the difference between coal and petroleum asphaltenes is not one of molecular size but one of molecular structure.

SUMMARY

Pocahontas (lvb) coal which is only sparingly (3 percent) soluble in hexamethylphosphoramide (HMPA) becomes 90 percent soluble when treated with a solution of lithium in HMPA. This high solubility is probably due to the formation of readily solvated aromatic anions of large volume; these anions are produced by the transfer of electrons from lithium to the aromatic nuclei in coal and readily react with alkylating agents such as ethyl iodide with addition of alkyl groups. The alkylated coal containing approximately one alkyl group per 5 carbon atoms is 86 percent soluble in benzene at room temperature. This method of alkylating coal is a new method for introducing functional groups into the coal molecule, it is not restricted to the use of HMPA as a solvent and should prove useful for modifying the physical and chemical properties of coal. The fact that introduction of alkyl groups into coal converts coal into a benzene soluble material points to a relationship between coal and petroleum asphaltenes and indicates that the difference between coal and petroleum asphaltenes is not one of molecular size but of molecular structure.

ACKNOWLEDGEMENTS

The authors wish to thank Janet L. Shultz for mass spectrometric and John Queiser for infrared analyses.

REFERENCES

1. De Boer, E. "Electronic Structure of Alkali Metal Adducts of Aromatic Hydrocarbons" in *Advances in Organometallic Chemistry*, F. G. A. Stone and R. West, Ed., Academic Press, New York, 1964.
2. Symposium on Electron Affinities of Aromatic Hydrocarbons and Chemistry of Radical Ions, Am. Chem. Soc., Div. Petroleum Chemistry, Preprints, April 1968, vol. 13, No. 2.
3. Normant, H. *Angew. Chem. Internat. Edit.*, 6, 1046 (1967).
4. Wawzonek, S. and Wearing, D. *J. Am. Chem. Soc.*, 81, 2067 (1959).
5. Cantrell, T. S. and Schechter, H. *J. Am. Chem. Soc.*, 89, 5868 (1967).
6. Cantrell, T. S. and Schechter, H. *J. Am. Chem. Soc.*, 89, 5877 (1967).
7. Scott, N. D., Walker, J. F., and Hansley, V. L. *J. Am. Chem. Soc.*, 58, 2442 (1936).
8. Gerdil, R. and Lucken, E. A. C. *Helv. Chim. Acta*, 44 1966 (1961).
9. Fraenkel, G., Ellis, S. H., and Dix, D. T. *J. Am. Chem. Soc.*, 87, 1406 (1965).
10. Sternberg, H. W., Markby, R. E., Wender, I., and Mohilner, D. M. *J. Am. Chem. Soc.*, 89, 186 (1967).
11. Winniford, R. S. and Bersohn, M. *Am. Chem. Soc., Div. Fuel Chem., Preprints*, Sept. 1962, 21-32; *C.A.*, 61, 509 (1964).
12. Friedel, R. A. and Retcofsky, H. "Proceedings of the Fifth Carbon Conference" Volume II, p. 149-165, Pergamon Press, New York, 1963.

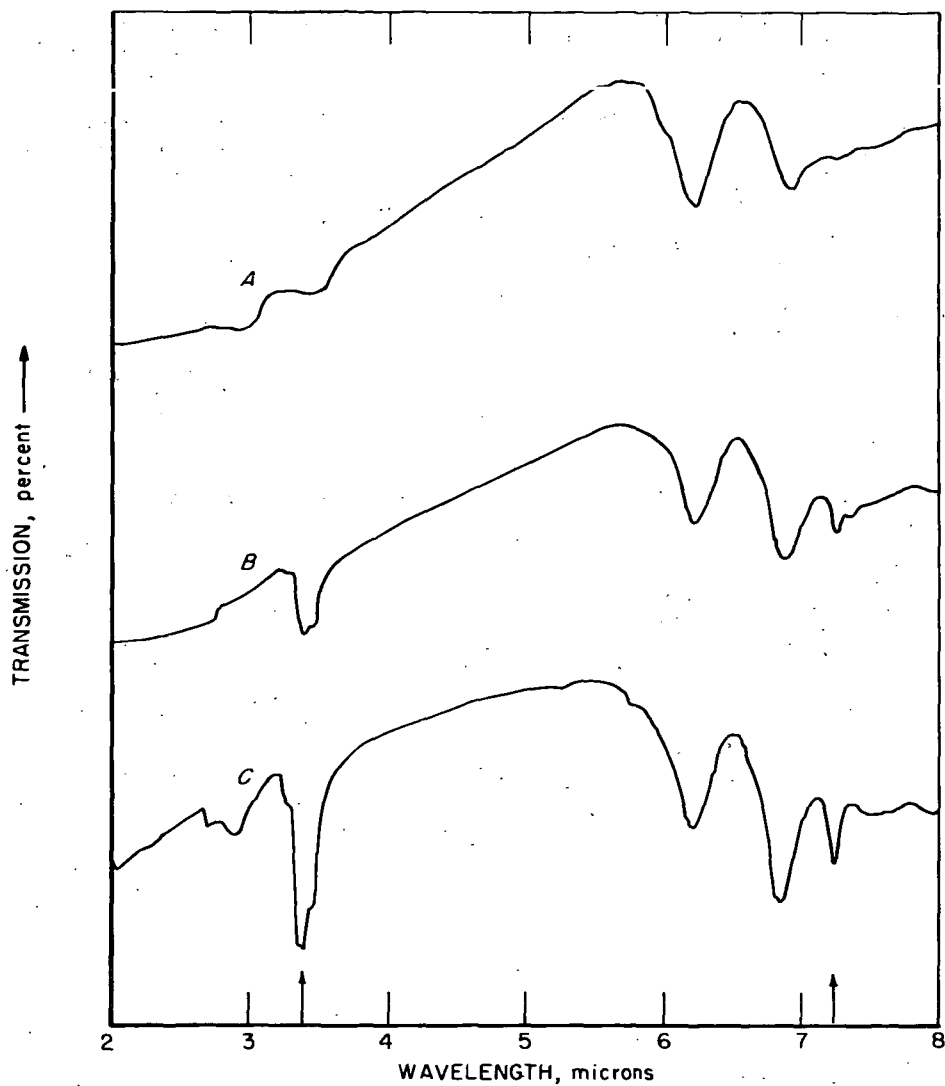


Figure 1.—Spectra of original and alkylated Pocahontas vitrains (*A*) original, (*B*) after one alkylation, (*C*) after two alkylations. Arrows indicate bands attributable to methyl group (7.25μ) and associated C-H stretching vibration (3.4μ).

L-10519

DESULPHURISATION OF COAL-OIL MIXTURES BY ATTRITION GRINDING
WITH ACTIVATED IRON POWDER*

Joseph Winkler

General Foam Division
Tenneco Chemicals, Inc.
Valmont Industrial Park
Hazleton, Pennsylvania 18201

INTRODUCTION:

Industrial progress and life itself inseparably depend on the quality of resources of water, land, and in particular, the air which we breathe. Air pollution, therefore, is of primary public concern and in all industrialized nations various steps are being undertaken to keep the air clean.

One of the main culprits of air pollution are fumes and gases from the combustion of fossile fuels. The principal toxic constituents of combustion gases are Sulphur Oxides from the Sulphur contained in Coal and in Fuel-Oils, derived from high-sulphurous crude oils. Excessive pollution of Air with combustion gases containing these sulphur oxides is understandably increasing with population growth, urbanisation and industrial expansion. No wonder, therefore, that in the United States, the 90th Congress passed the Air Pollution Bill No. 780 late in 1967 and has authorized close to a half billion dollars for a three-year program to combat Air Pollution. One of the points of this bill is for the U. S. Department of Health, Education, and Welfare to conduct Research on fuel beneficiation, leading to the elimination of Sulphur Oxides emission into the atmosphere.

To control air pollution caused by fumes and gases from combustion of high-sulphur fossile fuels, two basic approaches can be made:

1. To clean the combustion fumes and gases from Sulphur Oxides at their generation source prior to the release into the atmosphere;
2. To reduce the sulphur content of the fossile fuels BEFORE their combustion.

This short presentation is in the scope of the second approach, and I am attempting to show an economical, new way to remove Sulphur from Coal-Oil Mixtures.

I am fully aware that the experimental data presented herein is not conclusive and many questions remain to be answered by conducting of more detailed Research and Development work. This future work, however, should follow-up the present feasibility study in which, as it is given in the title of this lecture, organically bonded sulphur

• United States Patent 3,282,826 by Joseph Winkler

is being substantially removed from a Coal-Oil mixture by attrition grinding with activated powdery Iron.

Metals such as Iron, Nickel, Copper, Tin, Bronze, Lager Metal, etc. are capable to scavenge organically bonded sulphur from hydrocarbon type lube-oils under condition of friction. This has been well known for many decades.

For example, a lubricating oil which still contains some organically bonded sulphur because of insufficient refining, in use, very soon starts to show sludge formation. This sludge always analyzes for metallic sulphides.

It appears, therefore, that under high frictional forces occurring during the lubricating process in spite that the reactive surfaces of the contacting metallic surfaces are rather small and separated by a lubricating film, nevertheless, in time the organically bonded sulphur in the lubricating oil becomes slowly scavenged by the abraded minute metallic particles. In general, this phenomenon can be explained by the energetic preference of sulphur atoms to be bonded to metallic atoms rather than to carbon atoms.

As Metal Sulphides are insoluble in the lube-oil, this reaction proceeds further as the equilibrium preferred reaction.

When more favorable conditions are created, in which the used metal is in the form of a high surfaced fine powder, and its mixture with a sulphur containing oil-coal is most frequently and intimately attritionally mixed in a ball mill, it is obvious that in a shorter time a larger part of the organically bonded sulphur in the coal-oil mixture shall be scavenged by the metallic powder. The coal-oil mixture, from which molecules the sulphur atoms were abstracted, will under the reaction conditions partly depolymerise and partly polymerise, but in general a fluid fuel will result with a low sulphur content.

When this pasty reaction mixture is now diluted with a high boiling, good solvent, such as Tetralin* and centrifuged, the unreacted Metal and the Metal Sulphide having a relatively high specific gravity are easily separated from the reaction fluid, which now consists of an intimate dispersion of unreacted coal in an oily phase. After removal of the solvent, a low-sulphur, low-ash fuel results.

For the herein presented few exploratory experiments, the least expensive metal Iron Powder was used, although it might have been expected that Zinc, Tin, and Aluminum powders would perform better because of their higher atomic bond energy with Sulphur than Carbon.

However, the surface of Iron Powder easily becomes contaminated with reaction products with moist air, therefore, all commercial Iron Powders, even those which were made by hydrogen reduction have a partly oxidized surface. For that reason it was decided to prepare as much as possible a surface clean Iron Powder by the

* Tetralin - 1,2,3,4-Tetrahydronaphtalene - sp.gr. 60/60°F. = 0.971
m.p. = -30°C.; b.p. = 207°C.

following preactivation procedure:

A 0.1% benzene-absolute alcohol solution-dispersion of a mixture of three chemicals was percolated through the Iron powder.

This mixture consisted of a Cationic reducing wetting agent with an Organo-Tin compound doped with an Organo-Lead compound. (For patent reasons I do not feel free at this time to exactly identify these compounds.) After drying of the Iron powder in Nitrogen, it retained on the surface a plated-out, extra thin, metallic Tin film, whose weight was less than 0.05% of the weight of the Iron powder. Thus, what we really did was to deposit on the commercial Iron powder of a thin Tin-plate which, as we could observe under the microscope, was tenaciously adhering to the Iron powder surface even after the Iron powder was mixed into the coal-oil paste. This composition was applied with the expectation that the Tin plated Iron surface will initiate a Sulphur scavenging reaction, reminiscent of Melamid's Oil-Molten Tin cracking experience. The Tin plating of the Iron powder also appeared to prevent conglomeration of the Iron powder in the course of the grinding process.

Certainly, further considerable work should be done to explore how this really works and whether better wetting agents and activators can be found for that purpose. The use of radioactive tagging elements such as tritium and Fe_{59} incorporated into the wetting-activating compounds may elucidate their action.

EXPERIMENTAL:

I wish here to emphasize that the following presented herein few experiments should not give the impression that there is already on hand a developed method for Desulphurisation of Coal-Oil Mixtures. This is only a Feasibility Study in which I am only tentatively showing that by Attritional Grinding of a high-Sulphur containing paste made by solublizing Coal in Mineral Oil with a Sulphur Scavenging Metal such as inexpensive Iron powder, a quasi-metathetic reaction substantially appears to occur; this leading to a low-in-sulphur fuel, while producing Iron Sulphide as a commercially desirable by-product.

In order that this new method becomes inexpensive and practical, it should perform already at temperatures not much higher than 275°C.

Also the mixing-grinding reactor residence time should not be longer than 5 - 10 minutes. The reaction should also proceed preferably without the use of hydrogen because this requires high pressure working conditions. Hydrodesulphurisation is a too costly process for making a fuel only.

Finally, this new process should not produce appreciable amounts of low boiling volatiles resulting from high temperature decomposition of the oil and coal; this necessarily requiring a costly post-distillation step.

Only then, we may expect that the total production costs of a BTU shall be low enough to make it a practical desulphurisation method, competitive with the presently suggested H-oil process, which is using catalytic, high pressure hydrogenation of mineral oils.

Keeping all these considerations in view, for this limited feasibility study I have arbitrarily selected a conservative set of reaction constants, leaving for future much more extensive R & D work to find more efficiently working conditions:

The grinding time was five minutes at the grinding temperature of 250°C.

The grinder, equipped with a venting valve, was the well-known Union Process Company's Research Model Attritor No. 01.

This model has a grinding tank with a capacity of 750 cc. and delivered capacity of 200 - 400 cc.

To work at the intended high temperatures of 250 - 275°C., it was specially equipped with electrical wire heating and proper Teflon gasketing.

As grinding aids, steel balls of 15 mm. diameter were used.

The obtained from a supplier coal was predried and preground to an average 100 mesh. It was prepared from a high volatile coal grit, mined in the Mathies Mine in Washington county, near Pittsburgh, Pennsylvania. Its analysis after drying and grinding was:

Total Sulphur Content	1.70%	(of this, pyrite sulphur analyzed at 0.2%)
1. Moisture	0.10%	
2. Volatiles	39.00%	
3. Fixed Carbon	55.00%	
4. Ash	5.90%	
	<u>100.00%</u>	

The Iron Powder was a Niagara 100 mesh grade from the Pyron Company, a subsidiary of AMAX. It was an almost 100% pure hydrogen reduced Iron.

A constant weight ratio of 1:1 of coal powder to the solubilizing-grinding oil was kept in all experiments. At room temperature, depending on the physical and chemical properties of the used oil, the resulting mixture was a soft to firm paste. At the reaction temperature of 250°C. all these pastes were still thixotropic fluids evolving some volatile fumes; this again depending primarily upon its IBP and the composition and volatility of the used oil. The Fuel Oil No. 6 fumed the most because of its lowest IBP of only 489°F.

For our experiments we have selected four grades of grinding oils:

1. A high naphthenic, low in aromatics oil: Tufflo 6094 from Sinclair Oil Company. This oil analyzed: Aromatics - 8% and total sulphur - Less than 0.001%

2. A high aromatic oil: Mobilsol 66 from Mobil Oil Company. This oil analyzed: Aromatics - 95% and total sulphur - only 0.4%

3. A high aromatic oil: Aromatic RFC Extract and Concentrate from Enjay Chemical Company. This oil analyzed: Aromatics - 88% and total sulphur - 1.30%

4. A typical Fuel Oil No. 6 from Humble Oil and Refining Company. This oil analyzed: Aromatics - 65% and total sulphur - 2.60%

It is evident from the above and Table I, which gives a more complete analysis of these four grinding oils, that two highly aromatic oils were used, but one with a low and the other with a relatively high Sulphur content.

A third oil, Tufflo 6094, which is very low in aromatics and sulphur-free, was tested. It was interesting to test such an oil for its solubilizing power for the coal powder and consequently to find out what relatively the percentage of sulphur removal from the coal will result when dispersed and solubilized in such a poorly solvating oil.

Finally, for practical reasons a typical Fuel Oil No. 6 (Bunker Oil C) was included. This, first to establish its solubilizing power for a coal, and at the same time to tentatively find out whether our new process can substantially reduce the Sulphur content in such a coal-oil mixture to the desired below one percent.

Thus, with one type of a high volatile coal and four grades of grinding oil, four double basic experiments were run as follows:

Each grinding oil and the Coal-Iron powder were mixed: One batch while only using the agitator without the steel balls in the Attritor No. 01; the pairing batch was made with the steel balls. For this twin experiment all other conditions of time, temperature, and amount of ingredients, etc. were identical.

The results of these eight typical experiments are presented in Table II.

PROCEDURE:

Before their discussion I wish to detail the experimental procedure applied for any single run:

In a separate stainless steel one liter beaker, equal weight parts of the before described dried coal powder and the oil at a temperature of 100°C. were spatula mixed until a uniform paste resulted. To this paste a calculated amount of freshly activated Iron powder was admixed.

For each experiment the Iron powder was calculated on the basis of the average Sulphur content in the 1:1 oil-coal mix, sufficient to fully scavenge the Sulphur giving FeS. From this mixture a small known sample was removed and held back for analysis. When Steel Balls were used, these balls put into Attritor 01 up to about 25% of its volume; this while moving around the steel balls in the tank of the Attritor which was preheated to about 250°C. The also preheated to about 250°C. Coal-Oil-Iron Powder paste was added slowly--all while agitating the balls, thus filling-up all the free space between the balls until the total filled volume was about 75% and the average charge was 250 grams. When no steel balls were used, a steel double scraper with a tank wall tolerance of one millimeter was attached to the agitator and again the Attritor's tank was filled up to its 75% volume with the same Coal-Oil-Iron Powder mixture.

In all experiments, as indicated before, the volume of the scraper equaled the used volume of the steel balls.

The mixing time was, as before, 5 minutes while the reaction temperature was kept at 250°C. which, occasionally when steel balls were used climbed up to 275°C.--this mainly due to frictional heat.

After the reaction, the mixing and heating was discontinued and while hot the mixture was strained from the grinding balls (whenever they were used) and cooled to a temperature of about 150°C.

Four graduated 100 ml. centrifuge tubes were in the meantime filled to a half mark with Tetralin heated to 160°C. Into these tubes, while well mixing up to the 100 ml. mark the 150°C. hot, Coal-Oil-Iron powder reaction product was filled and all of the four tubes were centrifuged.

The centrifuge tubes were of the 3011-F45 type as depicted in Thomas Catalogue on page 221 with constricted neck and tampered bottom graduated from 0 to 1 in 0.05 ml., from 1 to 3 ml. in 0.2 ml., from 6 to 10 ml. in 0.5 ml., and 10 to 100 ml. in 1 ml. divisions.

The used centrifuge was the Explosion-Proof, International Model 2-EXD, as depicted in Thomas Catalogue on page 185. The centrifuging head for the tubes was the 2943-A15 type--each holding simultaneously four 100 ml. tubes, described above. The centrifuging speed was about 2100 rpm.

The centrifuge was not heated and centrifuging time was kept in all experiments at 5 minutes, while the centrifuging temperature fluctuated from the initial 150°C. to about 120°C. at the end due to intermittent cooling-off.

After centrifuging we could notice in the tubes four poorly visible layers:

1. In the bottom tip the unreacted blackish hard residue, which could be identified as Iron Powder, partly contaminated with Iron Sulphide.
2. On top of it, a black soft layer, identified as Iron Sulphide, partly contaminated with Coal particles.
3. On top of it an Oil-Tetralin-Coal deep brown viscous layer.
4. The upper top was a rather clear brown Oil-Tetralin solution.

Our main interest was to analyze the two upper liquid layers on its sulphur content, which was done in the following way:

When still hot the two upper layers were carefully decanted. Tetralin was added to the tube, well shaken, and again centrifuged. Afterwards, the upper liquid was again carefully decanted from the tube and this procedure was repeated once more. Thus, finally on the bottom of the centrifuge tube we had a Tetralin wet mixture of unreacted Iron Powder mixed with Iron Sulphide and sulphur-rich insoluble in Tetralin polymerisates. This Residue was carefully collected into a beaker, twice washed with Hexane and dried. From

this black powder the Iron particles as much as possible were magnetically removed and the remaining powder analyzed for Sulphur in a Parr Bomb by the usual BaSO_4 gravimetric method.

In all eight experiments we found a Sulphur content almost matching the Sulphur loss in the analyzed desulphurised oil-coal mixture.

The upper two layers from the centrifuges were mixed together with the Tetralin washings of the two lower layers, and Tetralin was distilled off from a small flask at about 200 - 210°C.

Finally we got a highly viscous, almost pasty, brown-black residue containing more or less suspended fine particulate coal; this depending upon the used grinding oil.

This residue was analyzed in a Parr Bomb for total sulphur. The results are presented on Table II.

In addition to these eight experiments a ninth experiment was made, in which the not activated Iron powder was used with the Coal-Fuel Oil No. 6 mixture. The comparative results are shown on Table III.

DISCUSSION AND CONCLUSIONS:

From the results shown on Tables II and III, we can tentatively make the following deductions:

1. Attritional grinding of a powdery high bituminous coal dispersed in a heavy mineral oil with Iron powder effected in five minutes at a temperature as low as 250°C. gives a higher degree of total sulphur removal than by conventional mixing. While for a straight mixing operation the Sulphur removal from three Coal-Oil mixtures averaged only 22%, attritional grinding with the same activated Iron Powder gave under otherwise identical working conditions a Total Sulphur removal as high as 53%.
2. Attritional grinding of a 1:1 dispersion of a high bituminous coal in Fuel Oil No. 6 with a non-activated Iron Powder and a specially activated Iron Powder gave a comparatively higher degree of Sulphur removal for the activated Iron Powder of 56% against 44% for the former.
3. For best Sulphur removal from Coal, the dispersing oil should contain predominantly aromatic compounds. This is shown clearly in Table II where two dispersing oils, one with an 8% aromatic content (Tufflo 6094), the other with 95% aromatic content (Mobilsol 66), were used for the same Coal. The first gave only an 11% Sulphur removal; the second gave 57% Sulphur removal.
4. The Sulphur removal from two Coal-Oil mixtures--the first being Mobilsol 66 which has a low Sulphur content of 0.4%, the second RFC Extract containing a triple percentage of Sulphur of 1.30%, give a similar percentage of removal of about 50%. This appears to imply that the Sulphur can be substantially removed not only from the Oil but also from the Coal, again provided that the Oil is of a highly aromatic type.

5. Mixtures of a Coal Powder, analyzing it at over one percent of total sulphur with a commercial Fuel Oil, which contains as high as 2.6% of organically bonded sulphur, can be desulphurised by the herein presented Attritional Grinding Method, while using a specially activated Iron Powder giving a down to less than one percent of Total Sulphur Fuel mixture.

FUTURE WORK:

The author believes that in R & D Work this process can be improved. This can be done by finding more favorable processing conditions. In particular, it is expected that by applying a higher reaction temperature and possibly increasing processing time over 5 minutes a higher degree of Sulphur removal can be attained.

It is also hoped that better Iron activators can be found--this may help in arriving at a lower in Sulphur Coal-Oil Fuel.

Further exploration of this new approach to Coal-Oil Desulphurisation appears worthwhile also for economical reasons. This because the expected processing conditions are rather mild, and the equipment for Grinding, Centrifuging, and Solvent Stripping are well developed and already available on an industrial scale. The high price of Sulphur, which by the presented method is produced as a by-product, should also contribute considerably to the lowering of processing costs.

TABLE I - PROPERTIES OF GRINDING OILS

Type of Grinding Oil	Tufflo 6094	Mobilsol 66	RFC Extract	Fuel Oil No. 6
Producer	Sinclair	Mobil	Enjay	Humble
Sulphur Content	None	0.4	1.3	2.6
Spec. Gr. 60/60°F.	0.9177	1.1050	1.054	0.969
Viscosity SSU at 100°F.	880	160	320	170
Viscosity SSU at 210°F.	190	38	62	35
Flash Point COC - °F.	425	385	405	180
ASTM Vac. Dist. (Cor. to Atm.)				
IBP	610	638	556	489
10%	780	697	644 (5%)	596
50%	821	724	776	927
90%	870 (95%)	793	1097	Cracked 971°F.
FBP	882	819	1126	Yield 62%
Clay/Gel Analysis				
Aromatics	8.0	95.0	88.0	65.0
Naphthenes + (Paraffin)	52 + (40)	1.0	10.0	12 + (8)
Polar Material	None	4.0	0.5	3.0
Asphaltenes	None	None	1.5	12.0
Carbon Type Analysis				
Aromatics Carbons	None			
Paraffinic Carbon	43			
Naphtenic Carbons	57			

TABLE II

Used Grinding Oil	Tufflo 6094	Mobilisol 66	RFC Extract	Fuel Oil No. 6
Analyzed total Sulphur content in the oil-coal mixture <u>prior</u> to the addition of the Iron Powder and before processing	0.85	1.05	1.50	2.15
Analyzed total Sulphur content in the oil-coal mixture after <u>only</u> mixing in the Attritor <u>01</u> without the steel balls	0.80 (or a re- duction in "S" content of 6%)	0.80 (or a re- duction in "S" content of 24%)	1.20 (or a re- duction in "S" content of 20%)	1.70 (or a re- duction in "S" content of 21%)
Analyzed total Sulphur content in the oil-coal mixture after attritional grinding with the steel balls	0.75 (or a re- duction in "S" content of 11%)	0.45 (or a re- duction in "S" content of 57%)	0.80 (or a re- duction in "S" content of 47%)	0.95 (or a re- duction in "S" content of 56%)

REMARKS:

In all experiments we could detect in the Residue, described in the text of this presentation, corresponding values of Sulphur which were scavenged with the Iron Powder.

TABLE III

Used Grinding Oil	Fuel Oil No. 6
Analyzed Total Sulphur Content in the Oil-Coal mixture after attritional grinding with the steel balls.	0.95 (or a reduction in "S" content of 56%)
The Iron powder was activated.	
Analyzed Total Sulphur Content in the Oil-Coal mixture after attritional grinding with the steel balls.	1.20 (or a reduction in "S" content of ONLY 44%)
The Iron powder was NOT activated.	

Some Pumping Characteristics of Coal Char Slurries

M. E. Sacks, M. J. Romney, and J. F. Jones

FMC Corporation, Chemical Research and Development Center
Princeton, New Jersey

As part of the program sponsored by the Office of Coal Research for increasing coal markets, Project COED (Char Oil Energy Development) is aimed at 1) developing an economic process for upgrading coal energy by converting coal to an oil, a gas, and a fuel char, and 2) decreasing the delivered cost of coal energy (1). One possible method for lowering the delivered cost of coal energy is to transport the char in a slurry to market. The pumping of solid fuels in a slurry is not new. Consolidation Coal Company demonstrated the feasibility of pumping coal-water slurries in a 108-mile coal pipeline (2). Char from a COED plant could be conveyed either in a water or oil slurry. Alternately, the char could be pumped in a water slurry with intermittent slugs of COED oil. The objective of this study was to obtain preliminary data in order to evaluate the technical feasibility of transporting char in a pipeline as a slurry.

The viscosity of char slurries was measured to determine the effects of char loading and size distribution. This survey was followed by extensive testing in an experimental pipeline.

Slurry Material

Water and two different oils--mineral oil and a petroleum recycle oil--were used as slurry media. The latter oil was used because it was similar to the product oil from a COED plant. The viscosities of the two oils were 36 and 8 cp at 100°F.

The char used for the slurries was obtained from pyrolysis of Utah A-seam coal in a multistage fluidized-bed process developed under Project COED (1). Its properties are listed in Table I.

Initial Viscosity Measurements

A rotating-spindle viscometer, Brookfield Model RVT, was used in these studies. The depth to which the spindle was inserted into the slurry, the time required for the measurement, and the temperature of the slurry were duplicated for each test. Slurry viscosities were determined at 100°F.

For char loadings higher than 25 weight percent, the viscosities of the two char-oil slurries were nearly the same, although the viscosities of the pure slurry media differed by a factor of 3.5 (Figure 1). The viscosities for the water slurries were lower at the same solids concentration.

The size consist of the char has a large effect on the observed viscosity of the slurry. Size consists for eight slurries are shown in Table II. The size distributions have two distinct peaks. One occurs between 16 and 100 mesh, and the other below 325 mesh. The average particle size was changed by varying the relative size of these two peaks. Test No. 8 is different from the others in that a large proportion of plus 16-mesh char is present with little material between 48 and 325 mesh. This slurry had a viscosity of 184 cp,

while the slurry in Test No. 4, which had the same average particle size, had a viscosity of 288 cp. Thus, a size distribution containing large and small particles, but no intermediate ones, may be desirable. This confirms the conclusions of Moreland (3) and Reichl (4).

Tests made on a 50 percent char-water slurry indicated that a minimum viscosity occurs when about one half of the char is minus 325-mesh material.

Some results of tests made employing different rotational speeds of the viscometer are given in Table III. These indicated that concentrated slurries exhibit non-Newtonian behavior. Further aspects of this non-Newtonian behavior will be discussed later.

Experimental Pipeline

A sketch of the pipeline used for testing the pumpability of char slurries is shown in Figure 2. The major components are:

1. A centrifugal pump with an open impeller and a 15 hp motor.
2. A 150-gallon slurry tank with an attached mixer for agitation.
3. A 55-gallon weigh drum for determining volumetric flow rates.
4. About 100 feet of 1-inch schedule 40 pipe arranged for recycle to the weigh tank or slurry tank.
5. Pressure-measuring devices consisting of diaphragm pressure seals, 6-inch dial gauges, and mercury manometers.

Known weights of char and slurry media were charged to the slurry tank and allowed to mix at least one hour before taking measurements to allow for absorption of the media in the pores of the char. Flow rates in the test section were controlled by by-passing a portion of the flow from the pump back to the slurry tank. Flow rates were determined by diverting the flow from the test section to a weigh tank. Average linear velocities ranged from 1 to 20 feet per second.

The pressure drop was measured over a 20-foot section with dial gauges and manometers. Pressure drops varied from 1 to 10 psi over the 20-foot section.

Pipeline Results

Figure 3 shows the effect of char concentration on pressure drop for char-mineral oil slurries at two linear velocities. Similar curves were obtained with char-water slurries. At low char loadings, the pressure drop increased only slightly over that of the liquid. After a certain loading was reached, however, the pressure drop rose very rapidly with further increases in char loading. The two oil slurries could no longer be pumped above a solids loading of 44 weight percent.

At low char loadings, the pressure drop obeyed the relationship:

$$\frac{\Delta P}{L} = k \bar{V}^a \quad (1)$$

The exponent was 1.72 for the two oil slurries, and 1.92 for the water slurries. This relation held for concentrations up to 25, 30, and 40 weight percent for the mineral oil, recycle oil, and water slurries, respectively, and for velocities as low as 3 ft./sec. The experimental data illustrating this relationship are shown in Figure 4. At higher concentrations the pressure drop was dependent on a smaller power of the velocity. This is an indication of the transition region between laminar and turbulent flow. However, dilute slurries could not be pumped in the laminar regime and concentrated slurries could not be pumped in the fully turbulent regime with the existing experimental equipment.

The effect of particle size on pressure drop was determined for char-water slurries. The addition of large amounts of minus 325-mesh char caused a marked decrease in the pressure drop, compared to that of a slurry with equal total solids loading but no fine material. Slurries with solids concentrations up to 50 percent were easily pumped. The quantitative effect of this fine material is shown in Figure 5 for two velocities at a total solids loading of 50 percent.

Discussion

An attempt was made to correlate the pipeline data on a friction factor-Reynolds number plot using the viscosity determined on the Brookfield viscometer. Such a correlation would be expected to exist, provided that the slurry can be described in terms of the properties of an equivalent fluid. The general shape of these plots were characteristic of the well known correlations for Newtonian fluids. The transition from laminar to turbulent flow was readily apparent. However, the quantitative results were not satisfactory. The transition to turbulent flow occurred at a Reynolds number of 1200 for char-mineral oil slurries and at a value of 600 for char-water slurries. In addition, the laminar data for the char-water slurries were not correlated by a single line. There was a definite trend towards higher friction factors with decreasing particle size (increasing minus 325-mesh). Hence, the effect of the size distribution was not completely accounted for by the equivalent Newtonian fluid properties of viscosity and density. This confirmed the non-Newtonian behavior indicated by the viscometer results.

A possible non-Newtonian model is the two-parameter Bingham fluid (5). This model gives the following relation between the shear stress and the shear rate:

$$\tau = -\eta \frac{du}{dr} + \tau_y \quad \tau > \tau_y \quad (2a)$$

$$\frac{du}{dr} = 0 \quad \tau < \tau_y \quad (2b)$$

This equation can be integrated (5) for pipe flow to give

$$q = (\bar{V}S) = \frac{\pi \Delta P R^4}{8\eta L} \left[1 - \frac{4}{3} \frac{\tau_y}{\tau_w} + \frac{1}{3} \left(\frac{\tau_y}{\tau_w} \right)^4 \right] \quad (3)$$

If the yield stress is small compared to the wall stress, the last term in the brackets may be neglected. Rearrangement and the insertion of $(\Delta P/L) R/2$ for the wall shear transforms Equation (3) into

$$\frac{\Delta P}{L} = 8 \left[\frac{\eta \bar{V}}{R^2} + \frac{\tau_y}{3R} \right] \quad (4)$$

The laminar data for char-water slurries are in agreement with this model. Pressure drop-velocity data were fitted to Equation (4). The resulting values of yield stress and plasticity are tabulated in Table IV.

The failure of the friction factor-Reynolds number plot to correlate the data can now be explained. The dimensional analysis leading to this correlation was based on only one rheological parameter, the Newtonian viscosity. If the two Bingham parameters are taken into consideration, a third dimensionless group is required (6, 7, 8). This is the Hedstrom number:

$$N_{He} = \frac{\rho \tau_y D}{\eta^2} \quad (5)$$

The Reynolds number is now based on the plasticity instead of the Brookfield viscosity:

$$N'_{Re} = \frac{\rho \bar{V} D}{\eta} \quad (6)$$

The data for char-water slurries in laminar flow were plotted using these dimensionless parameters in Figure 6. One set of data for char-oil slurries and a set for coal-oil slurries (9) are included. This correlation indicates that the Hedstrom number is about 1000, which is consistent with the value calculated from experimental yield stresses.

Some assumptions were required to obtain the curve for the turbulent region in Figure 6. At high shear rates, corresponding to turbulent flow,

$$-\eta \frac{du}{dr} \gg \tau_y$$

and Equation (2a) can be approximated by

$$\tau = -\eta \frac{du}{dr} \quad (7)$$

The slurries in turbulent flow can now be treated like Newtonian fluids.

An equation of the Blasius (5) form

$$f = k'' (N_{Re}')^b$$

was assumed for turbulent flow. Forcing Equation (1) into this form yields:

$$f = k' (N_{Re}')^{(a-2)} \quad (8)$$

Data from Figure 4 were transformed from the coordinates of head loss versus velocity to those of f versus N_{Re}' by using Equation (8). The error introduced by these approximations was never more than 20 percent. The result is a reasonable representation of the turbulent regime in Figure 6.

The most significant aspect of this correlation is the predicted suppression of turbulence at high Hedstrom numbers. Since the Hedstrom number is proportional to the square of the pipe diameter, it becomes increasingly important when attempting scale-up.

Economics

From the predictions of the correlation in Figure 6 and the properties of the slurries studied, a preliminary estimate of pumping cost was obtained. Figure 7 shows the estimated cost on a cents per ton per mile basis as a function of pipe diameter. Only those costs which are dependent on pipe diameter are included. At the diameter corresponding to the minimum in the total cost curve, the pumping cost is 0.16 cents per ton per mile. This is comparable to the operating costs of other commercial slurry pipelines (2).

In the final economic evaluation, several other factors need to be considered. The costs in Figure 7 do not include terminal facilities. These include not only capital investment in pumping stations, but slurry preparation and separation facilities as well. The effect of the extra fine material, which must be added, on product value has not been determined.

Acknowledgment

The authors thank the Office of Coal Research, Department of the Interior, and the FMC Corporation for permission to publish this paper. The authors also thank C. R. Allen for performing the initial work, and C. A. Gray for counsel during the investigation.

References

1. Jones, J. F., Eddinger, R. T., and Seglin, L., CEP, 62, 2, 73-79 (1966).
2. Reichl, E. H. and Thager, W. T., "Economics and Design Requirements of Pipeline Transport for Coal Slurry", Paper No. CPA 62-5113, National Power Conference, September, 1962.
3. Moreland, C., "Viscosity of Suspensions of Coal in Mineral Oil", The Canadian Journal of Chem. Engr., February, 1963.
4. Reichl, E. H., "Transportation of Coal by Pipelines", U. S. Patent No. 3,073,652 (1963).
5. Bird, R. B., Stewart, W. E. and Lightfoot, E. N., Transport Phenomena, John Wiley and Sons, Inc., New York-London (1960).
6. Thomas, David G., Ind. Eng. Chem., 55, 11, 18-29 (1963).
7. Ibid, 55, 12, 27-35 (1963).
8. Michiyoshi, I., Matsumoto, R., Mizuno, K., and Nakai, W., International Chemical Engineering, 6, 2, 383-8 (1966).
9. Berkowitz, N., "Some Newer Concepts in Solids Pipelining", Contribution No. 199 from the Research Council of Alberta, Edmonton, Canada (1963).

Nomenclature

a	Constant defined in Equation (1). Dimensionless
b	Constant
D	Pipe diameter, ft.
f	Fanning friction factor = $\frac{D}{4} \frac{\Delta P/Lg_c}{1/2\rho V^2}$ Dimensionless
k	Constant defined in Equation (1)
k'	Constant defined in Equation (8)
k''	Constant
L	Pipe length, ft.
N_{He}	Hedstrom number = $\frac{\rho\tau_y D^2}{\eta^2}$ Dimensionless
N'_{Re}	Modified Reynolds Number = $\frac{\rho\bar{V}D}{\eta}$ Dimensionless
ΔP	Pressure drop, psi
q	Volumetric flow rate, cu.ft./hr.
r	Radial distance, ft.
R	Pipe radius, ft.
S	Pipe cross sectional area, sq.ft.
u	Linear velocity, ft.sec. ⁻¹
\bar{V}	Average linear velocity, ft. sec. ⁻¹
$\frac{du}{dr}$	Shear rate, sec. ⁻¹
η	Plasticity defined by Equation (2a), lb _f sec.ft. ⁻²
ρ	Density, lb _m ft. ⁻³
τ	Shear stress, lb _f ft. ⁻²
τ_w	Shear stress at the wall = $\frac{P(R)}{L(2)}$ lb _f ft. ⁻²
τ_y	Yield stress defined by Equation (2a) lb _f ft. ⁻²

TABLE I
Physical Properties of Char

Properties	Before Pumping	After Pumping	
		Mineral Oil	Recycle Oil
Slurry Medium			
Density			
Bulk, lb./cu.ft.	27	34	-
Packed, lb./cu.ft.	31	41	-
Particle, g./cc.	0.79	-	-
Sieve Analysis, Tyler Mesh, cum. wt. %			
14	4	1	3
28	27	11	25
48	60	41	58
100	82	68	83
200	95	80	95
325	98	85	99
Average Particle Diameter, in.	0.009	0.005	0.009

TABLE II
Effect of Minus 325-Mesh Char Content on the Viscosity of a Char-Oil Slurry

Test No.	Char Size Consist. wt. % on Tyler Screen							Average Particle Diameter, in.	Viscosity of a 44 wt. % Char-Oil Slurry at 100°F., cp.
	16	28	48	100	200	325	Minus 325		
1	5.6	21.2	36.8	23.4	10.8	1.3	0.9	0.00739	616
2	5.1	19.3	33.4	21.2	9.8	1.2	10.0	0.00447	344
3	6.0	19.0	30.0	14.0	9.0	4.0	17.0	0.00344	328
4	4.5	17.1	29.7	18.9	8.7	1.1	20.0	0.00323	288
5	4.0	15.0	26.0	16.5	7.6	0.9	30.0	0.00252	250
6	3.4	12.8	22.3	14.2	6.5	0.8	40.0	0.00205	180
7	0.3	11.0	26.4	17.6	10.6	6.6	27.5	0.00245	202
8	31.0	20.5	12.0	6.1	2.6	1.1	26.5	0.00310	184

TABLE III

Viscosity of a 40 Weight Percent Char-Water Slurry
at Different Rotational Speeds of Viscometer

<u>Rotational Speed, rpm</u>	<u>Apparent Viscosity Measured With a Brookfield RVT Viscometer Using Spindle No. 2</u>
100	132
50	260
20	455

TABLE IVRheological Parameters

<u>Nominal Total Solids Concentration, wt. %</u>	<u>Minus 325- Mesh Char Concentration, wt. % of total solids</u>	<u>Yield Stress, τ_y lb_f/sq.ft. $\times 10^2$</u>	<u>Plasticity or Limiting Viscosity, η lb_f.sec./ sq.ft. $\times 10^4$</u>	<u>Measured Total Solids Concentration, wt. %</u>
50 char in water	47.5	4.13	5.84	50.4
	41.9	6.42	5.85	51.6
	36.9	2.53	8.02	47.4
	34.8	7.01	7.67	48.9
	28.6	5.27	10.52	52.3
45 char in water	28.6	5.49	6.55	45.4
38 char in recycle oil	-	(-6.96)	21.8	-
55 coal in oil	-	0.276	11.88	-

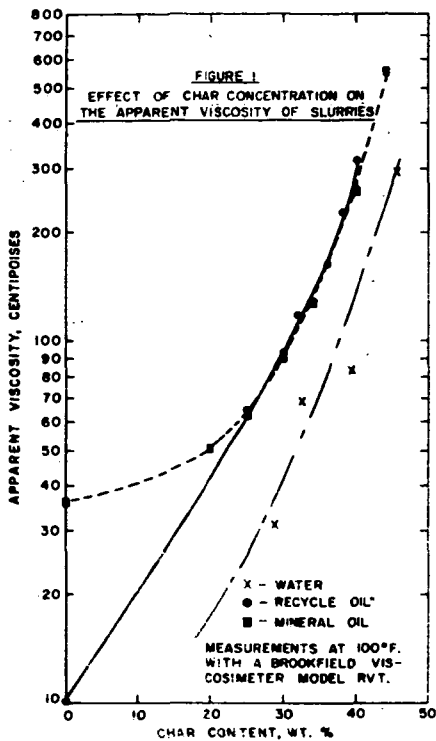
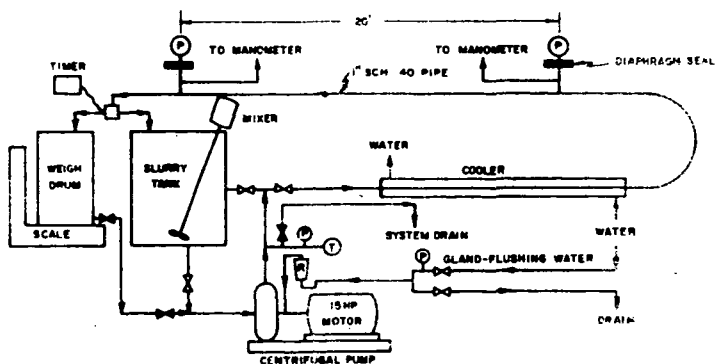


FIGURE 2
PIPELINE TEST SYSTEM



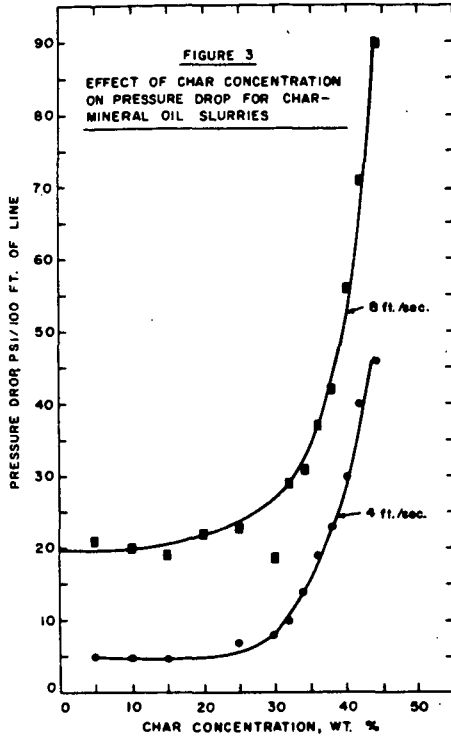


FIGURE 4
HEAD LOSS VERSUS VELOCITY FOR CHAR-WATER SLURRIES WITH SOLIDS CONCENTRATIONS FROM 21 TO 39 WEIGHT PERCENT

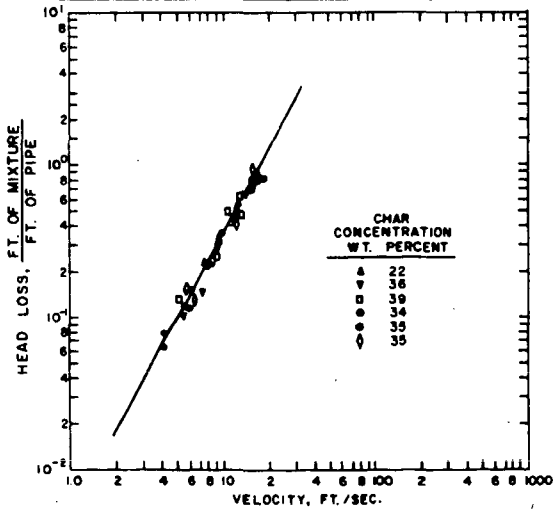


FIGURE 5
EFFECT OF CONTENT OF MINUS 325-MESH
CHAR ON PRESSURE DROP
FOR A 50-50 CHAR-WATER SLURRY

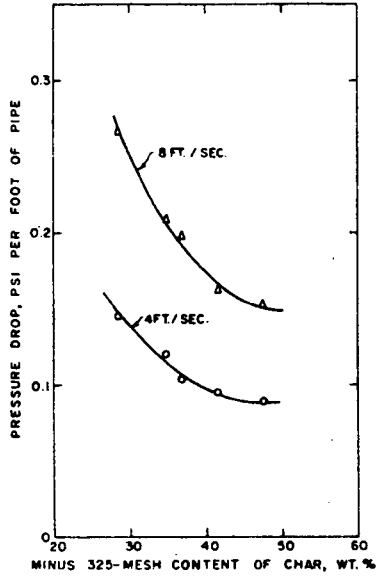


FIGURE 6
MEDSTROM NUMBER-REYNOLDS NUMBER-FRICTION FACTOR PLOT

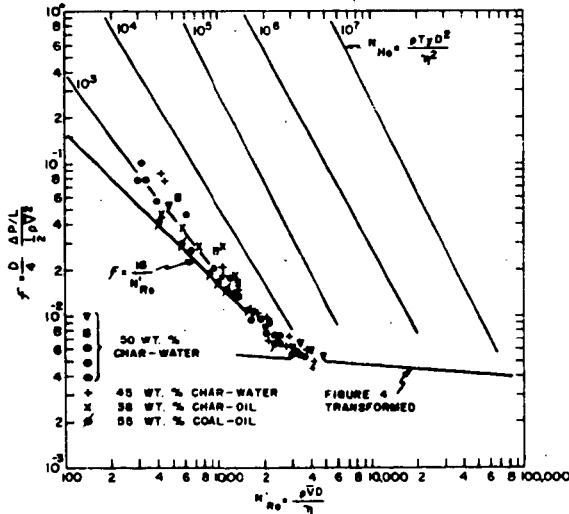
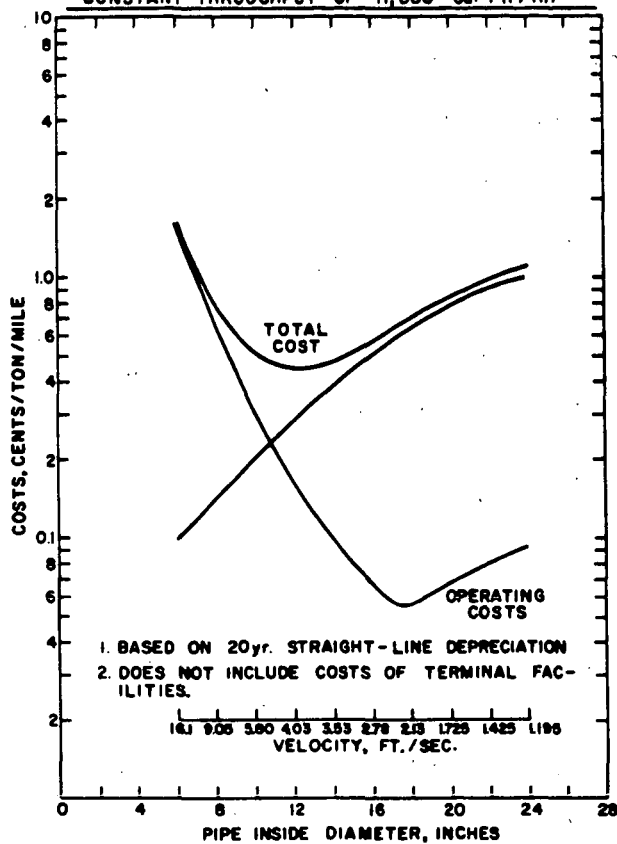


FIGURE 7
PIPE DIAMETER VERSUS COST OF PIPELINING FOR A
CONSTANT THROUGHPUT OF 11,380 Cu. Ft./Hr.



CONTROLLED LOW-TEMPERATURE PYROLYSIS OF BENZENE-EXTRACTED GREEN RIVER OIL SHALE

J. J. Cummins and W. E. Robinson

Laramie Petroleum Research Center
Bureau of Mines, U.S. Department of the Interior
Laramie, Wyoming 82070

INTRODUCTION

The present study was undertaken to determine the rate at which oil-shale kerogen decomposes and to determine the composition of the pyrolytic products formed at 300° and 350° C in a helium atmosphere at atmospheric pressure. A study of the thermal reaction at these low temperatures (150° to 200° C below normal retorting temperatures) is important because of the current interest in the in situ retorting processes of converting oil shale to shale oil. During in situ retorting it may take long periods of heating to raise the temperature of the oil shale from ambient temperature to the final retorting temperature, thus thermal reactions at intermediate temperatures may become important. The present study was made to investigate some of the possible variables in the thermal behavior of the oil-shale organic material as a function of time and temperature.

A number of investigators have studied the conversion of oil shale to pyrolytic products. Hubbard and Robinson⁶ investigated the oil-shale decomposition rates from 350° to 500° C. Dinneen³ studied the effect of various retorting temperatures on the composition of shale oil. Allred¹ presented some considerations on the kinetics of oil-shale pyrolysis. Hill and co-workers⁵ studied the thermal decomposition of kerogen in the presence of methane.

The present study extends the published data to a lower temperature range by discussing the kinds of products obtained at pyrolysis temperatures of 300° and 350° C and at pyrolysis times ranging from 12 to 96 hours.

EXPERIMENTAL

One-hundred-gram samples of benzene-extracted oil shale were heated at 300° or 350° C for selected periods of 12, 24, 48, 72, or 96 hours in a helium atmosphere at atmospheric pressure. The amounts of pyrolytic products that formed during the heating process (except gas and carbon residue) were determined. No attempt was made to determine the amount of gas and carbon produced because only small amounts are formed at these temperatures. The pyrolytic product that volatilized during the heating is called oil. The pyrolytic product that did not volatilize was recovered by extracting the heated residue and is called bitumen.

Oil-Shale Sample. The sample of Green River oil shale used in this study was obtained from the Bureau of Mines demonstration mine near Rifle, Colorado. The sample assayed about 66 gallons of oil per ton of shale, contained 30.2 percent organic carbon, and contained 7 percent benzene-soluble bitumen. Prior to heating, the shale was crushed to pass a 100-mesh sieve and then benzene extracted five times, each time with fresh solvent, until it was essentially free of soluble organic material. This was demonstrated by the decreasing recovery with each successive extraction. The extracted sample was then dried at 60° C under reduced pressure until free of benzene.

The percent organic carbon in the extracted oil shale and in the pyrolytic residues was determined by combustion analysis. The results were used as a measure of the kerogen decomposition.

Apparatus. The pyrolysis apparatus used in this investigation is capable of heating a 100-gram sample of oil shale. Weighed samples were pyrolyzed in a stainless-steel boat housed in a Pyrex combustion tube 800-mm long x 50-mm o.d. One end of the combustion tube was equipped with a metal cap having a sliding metal bar through the middle of the cap and a gas inlet tube in the side of the cap. The metal bar was used to move the boat in or out of the hot zone of the furnace. The other end of the combustion tube was connected to two traps in series, a water-cooled trap followed by a Dry Ice trap.

Recovery of the Products. The volatile product (oil) that condensed in the water-cooled trap was recovered with benzene. After the benzene was removed, the product was dried and weighed. The heated residue was cooled in the outer end of the combustion tube in the presence of helium. After cooling, the heated residue was placed in a Soxhlet extractor and extracted with benzene for 16 hours. The nonvolatile product (bitumen) recovered from the benzene solution by evaporation of the benzene, was dried and weighed. The residue was dried under vacuum at 60° C and weighed. The percent organic carbon remaining in the heated residue was determined, and the percent unconverted organic carbon was calculated from this determination and from the results of a similar determination on the starting material. Most of the pyrolytic gases were trapped in the Dry Ice trap. The trap was allowed to warm to room temperature. The weight of the product was used to estimate the amount of gas formed.

Fractionation of the Oil and Bitumen. Each oil and each bitumen were fractionated using standard procedures.² The product was allowed to stand in pentane at 0° C for 16 hours thereby separating the material into pentane-soluble and pentane-insoluble fractions. After the pentane was removed, the pentane-soluble material was placed on an alumina column using a 1 to 25 ratio of sample to alumina and was fractionated by elution chromatography into hydrocarbon concentrate and resin fraction. The hydrocarbon concentrate was placed on a silica-gel column, using a 1 to 25 ratio of sample to silica gel, and separated into an alkanes-plus-olefins fraction and an aromatic-oil fraction. The alkanes plus olefins were placed on a silica-gel column using a 1 to 60 ratio of sample to silica gel and fractionated into alkane and olefin fractions using a method developed by Dinneen and co-workers.⁴ The alkanes were placed on 5 Å molecular sieves and separated into an n-alkane fraction and a branched-plus-cyclic alkane fraction. The n-alkanes were fractionated using a programmed GLC at a heating rate of 7.5° C min⁻¹ and using a 5-foot, 1/4-inch SE 30 column.

RESULTS AND DISCUSSION

The results of this study will be discussed in terms of the amount of pyrolytic products formed, the conversion of kerogen to oil and bitumen, and the order of thermal reactions. In addition, the distribution of individual components of the thermal products and their rates of formation will be discussed. As an aid to planning future studies, the conversion of kerogen to pyrolytic products at temperatures lower than 300° C was estimated.

At low temperatures kerogen is converted mainly to oil and bitumen. The amount of gas formed at 300° and 350° C was less than 1 percent of the total pyrolytic products. The amount of carbon residue formed at 300° and 350° C, although not determined, was assumed to be less than 1 percent of the pyrolytic product. Thus, the pyrolytic gas and carbon residue formed were

not considered separately in this report. Any carbon residue formed was included in the unconverted kerogen value and any gas formed was included in the kerogen converted value.

The amounts of pyrolytic products formed at 300° and 350° C at different time intervals appear in table 1. The percent of the kerogen converted to pyrolytic products is based on the

TABLE 1. - The amount of pyrolytic products formed

Time, hours	$(100X)^{1/2}$	1-X	Log (1-X)	Weight percent of pyrolytic products	
				Oil	Bitumen
300° C					
12	5.4	0.946	-0.0241	73	27
24	7.4	.926	- .0334	69	31
48	8.6	.914	- .0391	77	23
72	9.7	.903	- .0443	78	22
96	11.0	.890	- .0506	76	24
350° C					
12	34.9	.651	- .1864	62	38
24	40.2	.598	- .2233	63	37
48	51.4	.486	- .3134	72	28
72	61.8	.382	- .4179	77	23
96	64.3	.357	- .4473	94	6

$1/2$ Kerogen converted, weight percent of total kerogen.

difference between the organic carbon content of the sample before heating and the organic carbon content of the heated residue after the removal of the volatile and soluble products. At each temperature, the amount of kerogen converted to pyrolytic products doubled when the heating time was increased from 12 to 96 hours. Approximately a sixfold increase in the amount of kerogen converted was obtained when the temperature was increased from 300° to 350° C.

The kerogen is converted to a volatile oil product and to a nonvolatile bitumen during pyrolysis. At both temperatures the amount of volatile oil formed is greater than the amount of bitumen formed. A large decrease in the amount of bitumen was obtained at 96 hours over that obtained at 72 hours at 350° C. This indicates that the bitumen degraded and volatilized as oil.

The conversion of kerogen to oil and bitumen at 300° C is shown in Figure 1 where concentration is plotted against time. The oil-plus-bitumen curve rises sharply for the first 24 hours, then tends to level off from 24 to 96 hours. Similar trends are apparent in the oil and bitumen curves. These trends suggest that the conversion of bitumen to oil is negligible at 300° C. In contrast, a similar plot of the 350° C data (Figure 2) shows that the bitumen curve decreases after 72 hours and tends toward zero at 96 hours. The oil curve continues to rise between 72 and 96 hours. The latter results support the findings of Allred¹ and Hubbard and Robinson⁶ who suggest that kerogen is converted to bitumen and the bitumen is in turn converted to oil.

To determine the order of the thermal reaction of kerogen at 300° and 350° C, the log of the kerogen concentration [$\log(1-X)$ shown in table 1] was plotted against time for each temperature. Reasonably straight line relationships were obtained for the 300° C data (Figure 3) and the 350° C data (Figure 4) showing that the overall thermal conversion of kerogen at these temperatures is probably first order.

The specific reaction rates at each temperature were calculated from the slope of the curves in the log concentration-time plots and equal 2.303 times the slope of the curve. The determined specific reaction rate (k) of the total thermal product at 300° C equals 0.7×10^{-3} hour⁻¹ and at 350° C equals 7.6×10^{-3} hour⁻¹. From this, it appears that the reaction rate at 350° C is about 11 times the rate at 300° C. The calculated activation energy between 300° and 350° C is about 33 kilocalories mole⁻¹.

Each oil and each bitumen were fractionated to ascertain any existing differences in their compositions. The oils and bitumens were fractionated into the following type components: n-Alkanes, branched-plus-cyclic alkanes, olefins, aromatic oil, resins and pentane-insoluble material. The distribution of these fractions appears in table 2 where the results obtained for

TABLE 2. - Distribution of components present in the thermal product

Time, hours	Weight percent of kerogen					Pentane- insoluble material
	n-Alkanes	Branched-plus- cyclic alkanes	Olefins	Aromatic oil	Resins	
300° C						
12	0.17	0.30	0.05	0.17	4.00	0.71
24	.11	.71	.17	.17	2.93	3.31
48	.13	.79	---	.43	7.05	.20
72	.15	1.00	.15	.61	7.14	.65
96	.26	1.02	.19	1.02	8.01	.50
350° C						
12	.80	2.48	.56	1.95	25.93	3.18
24	2.17	3.70	.64	3.38	25.97	4.34
48	1.39	3.86	.36	1.75	35.87	8.17
72	2.72	3.52	.80	1.17	35.98	17.61
96	3.02	4.82	1.22	4.24	48.24	2.76

the volatile oil and the nonvolatile bitumen were calculated as one pyrolytic product. In general, the thermal products from both temperatures contained more polar materials (resins plus pentane-insoluble materials) than hydrocarbons.

The data from the fractionation of the oils and bitumens prior to combining showed the oil fractions to contain more hydrocarbons than did the bitumen fractions. The hydrocarbon content of the oil fractions ranged from 20 to 26 percent of the total fraction, and the hydrocarbon content of the bitumen fractions ranged from 1 to 7 percent. These results show that during oil-shale

pyrolysis the high-molecular-weight nonvolatile polar bitumen degrades to a less polar and lower-molecular-weight oil. These results are different than those from a previous study⁶ where kerogen was pyrolyzed at 350° C in tetralin to soluble products. In that study more than half of the products remained as high-molecular-weight pentane-insoluble material. This indicated that further degradation to volatile products is not a major factor when kerogen is converted to pyrolytic products in the presence of tetralin.

The specific reaction rates were calculated for the individual components of the pyrolytic products using the method previously described. The results are shown in table 3. At

TABLE 3. - Reaction rates for the production of the individual components present in the thermal products

Fraction	k, hours ⁻¹		$\frac{350^\circ \text{ C rate}}{300^\circ \text{ C rate}}$
	300° C	350° C	
n-Alkanes	3×10^{-5}	6×10^{-4}	20
Branched-plus-cyclic alkanes	1×10^{-4}	3×10^{-4}	3
Olefins	1×10^{-4}	7×10^{-4}	5
Aromatic oil	9×10^{-5}	4×10^{-4}	4
Resins	5×10^{-4}	4×10^{-3}	8
Pentane-insoluble material	2×10^{-4}	2×10^{-3}	9
Total product	1×10^{-3}	8×10^{-3}	7

300° C the n-alkanes are formed at the slowest rate while the resins are formed at the fastest rate. At 350° C the branched-plus-cyclic alkanes are formed at the slowest rate while the resins are formed at the fastest rate. The total product rate agrees favorably with the overall rate given previously. The 350° C rate divided by the 300° C rate shows the proportional rate of increase of the individual components between 300° and 350° C and their relationship to the overall rate. Normal alkanes formed 20 times as fast at 350° C as at 300° C. Branched-plus-cyclic alkanes formed three times as fast at 350° C as at 300° C. The change in production of the other fractions is not much different from the change in the total product rate.

The n-alkanes from the oil fractions were separated by GLC and chromatograms were obtained for each fraction. Plots of carbon numbers of the n-alkanes versus concentration were made to determine the effect of pyrolytic time and temperature on the composition of the n-alkanes. The data from the 300° C n-alkanes produced envelopes at C₁₃ to C₂₆ and envelopes at C₂₇ to C₃₅. The data from the 350° C alkanes produced envelopes at C₁₂ to C₂₆ and C₂₇ to C₄₀. In general, the percent of n-alkanes in the C₁₂ to C₂₆ range increased with increase in heating time at both temperatures. Also, the percent of n-alkanes in the C₂₇ to C₄₀ range decreased with increase in heating time at both temperatures. These results indicate that more low-molecular-weight n-alkanes than high-molecular-weight n-alkanes are thermally degraded from the kerogen or degraded from the bitumen with increased time and temperature.

A plot of percentage of kerogen converted, in terms of the yearly rates ($R \times 10^2$), versus the reciprocal of absolute temperature was made to determine if it is practical to study the thermal reaction rate of kerogen at temperatures lower than 300° C. The plot (Figure 5), based on the thermal reaction rate per year at 300° and 350° C, is extrapolated to 50° C. The figure shows that 100 percent of the kerogen would be converted to soluble products in 1 year at 265° C.

About 30 percent of the kerogen would be converted to soluble products in 1 year at 250° C while about 1 percent would be converted in 1 year at 200° C. It is evident from this plot that extended periods of time would be required to study the rate of conversion at temperatures lower than 300° C. One interesting aspect of this plot is the indication that about 6 percent of the kerogen should be converted to soluble products at 50° C in 100 million years. This suggests that the soluble bitumen present in the oil shale could have been derived from the kerogen at temperatures as low as 50° C during the life span of the Green River Formation (Eocene, 60 million years).

SUMMARY

A twofold increase was obtained in the amount of pyrolytic product at constant temperature (300° or 350° C) when the length of heating time was increased from 12 to 96 hours. A sixfold increase was obtained in the amount of pyrolytic product at constant heating time when the temperature was increased from 300° to 350° C.

The overall thermal decomposition of kerogen at 300° and 350° C appears to be a first-order reaction. The specific reaction rate constant at 300° C was determined as 0.7×10^{-3} hour⁻¹ and at 350° C as 7.6×10^{-3} hour⁻¹.

Differences in the rate of formation of individual type components of the pyrolytic product are apparent. Between 300° and 350° C, n-alkanes formed faster than the overall average rate of product formation while the branched-plus-cyclic alkanes formed slower than the overall average rate. Rate of formation of the other fractions was nearly equal to the average rate.

The average molecular weight of the n-alkane fraction decreased with increase in heating time and heating temperature.

Extrapolation of the rate data to temperatures below 300° C indicated that the amount of natural bitumen present in oil shale could have been thermally degraded from kerogen at 50° C in a period of time equivalent to the estimated age of the Green River Formation.

ACKNOWLEDGMENT

The work upon which this report is based was done under a cooperative agreement between the Bureau of Mines, U.S. Department of the Interior and the University of Wyoming.

REFERENCES

1. Allred, V. D. Some Considerations on the Kinetics of Oil Shale Pyrolysis. Presented at the Symposium on Oil Shale and Shale Oil Processing, Fifty-Eighth National A.I.C.E. Meeting, Dallas, Texas, February 1966.
2. Cummins, J. J., and W. E. Robinson. Normal and Isoprenoid Hydrocarbons Isolated from Oil-Shale Bitumen. *J. Chem. Eng. Data*, v. 9, No. 2, 1964, pp. 304-307.
3. Dinneen, G. U. Effects of Retorting Temperature on the Composition of Shale Oil. *Chem. Eng. Progr.*, v. 61, No. 54, 1965, pp. 42-47.

4. Dinneen, G. U., J. R. Smith, R. A. Van Meter, C. S. Allbright, and W. R. Anthony. Application of Separation Techniques to a High Boiling Shale-Oil Distillate. *Anal. Chem.*, v. 27, 1955, p. 185.
5. Hill, G. R., D. J. Johnson, L. Miller, and J. L. Dougan. Direct Production of a Low Pour Point High Gravity Shale Oil. *Ind. and Eng. Chem., Product Research and Development*, v. 6, No. 1, 1967, pp. 52-59.
6. Hubbard, A. B., and W. E. Robinson. A Thermal Decomposition Study of Colorado Oil Shale. *BuMines Rept. of Inv. 4744*, 1950, 24 pp.
7. Robinson, W. E., and J. J. Cummins. Composition of Low-Temperature Thermal Extracts from Colorado Oil Shale. *J. Chem. Eng. Data*, v. 5, 1960, pp. 74-80.

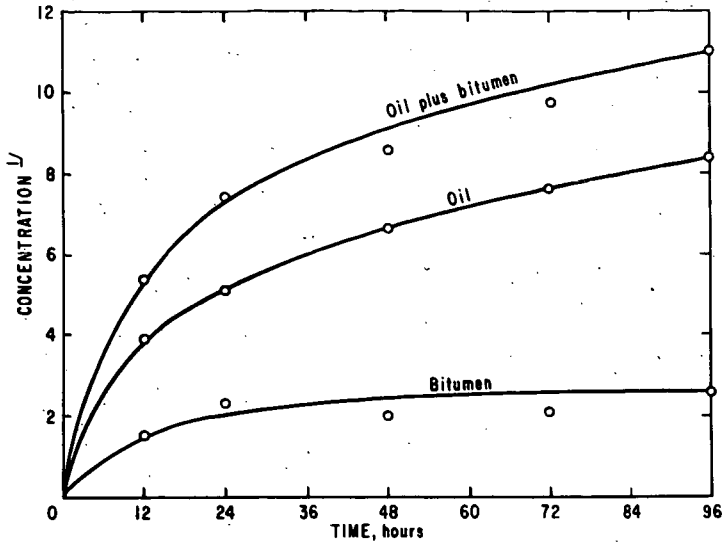


FIGURE 1.-Conversion of Kerogen to Oil and Bitumen at 300 °C.
(% Kerogen converted, wt pct of total kerogen)

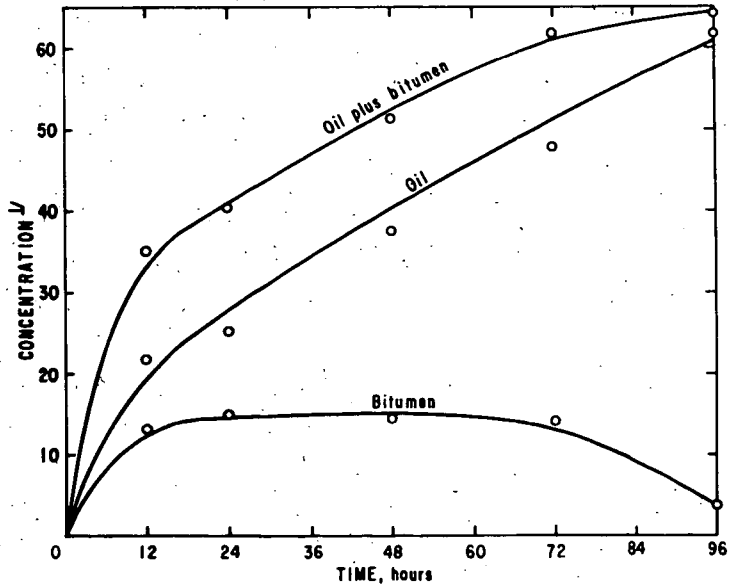


FIGURE 2.-Conversion of Kerogen to Oil and Bitumen at 350 °C.
(% Kerogen converted, wt pct of total kerogen)

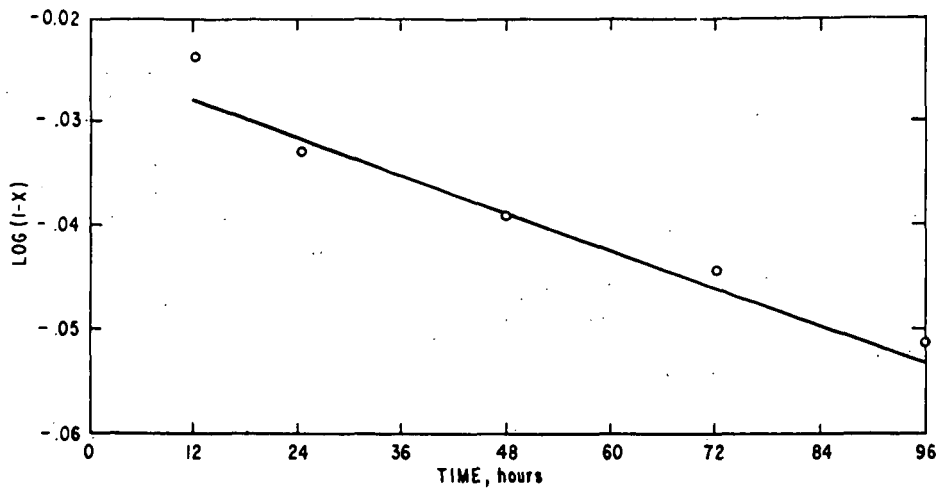


FIGURE 3.-First-Order Plot of Kerogen Conversion at 300 °C.

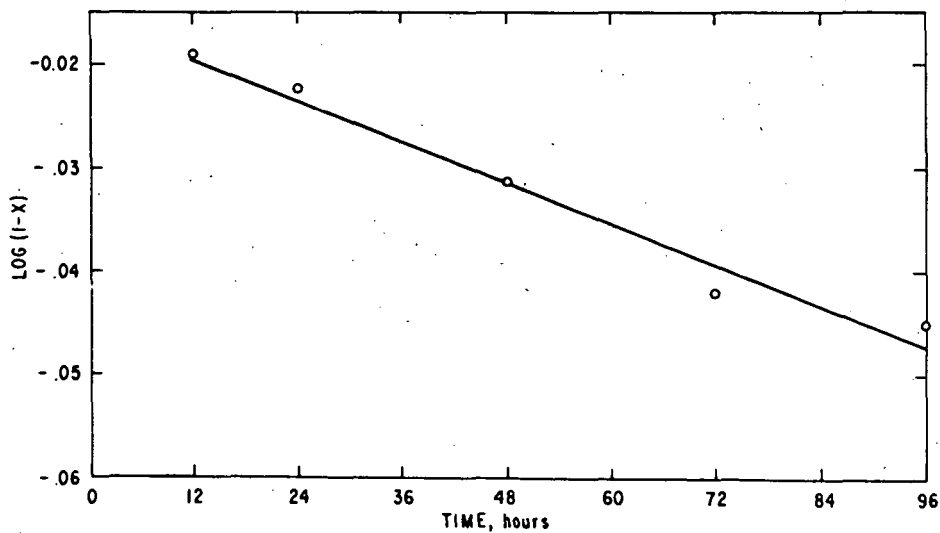


FIGURE 4.-First-Order Plot of Kerogen Conversion at 350 °C.

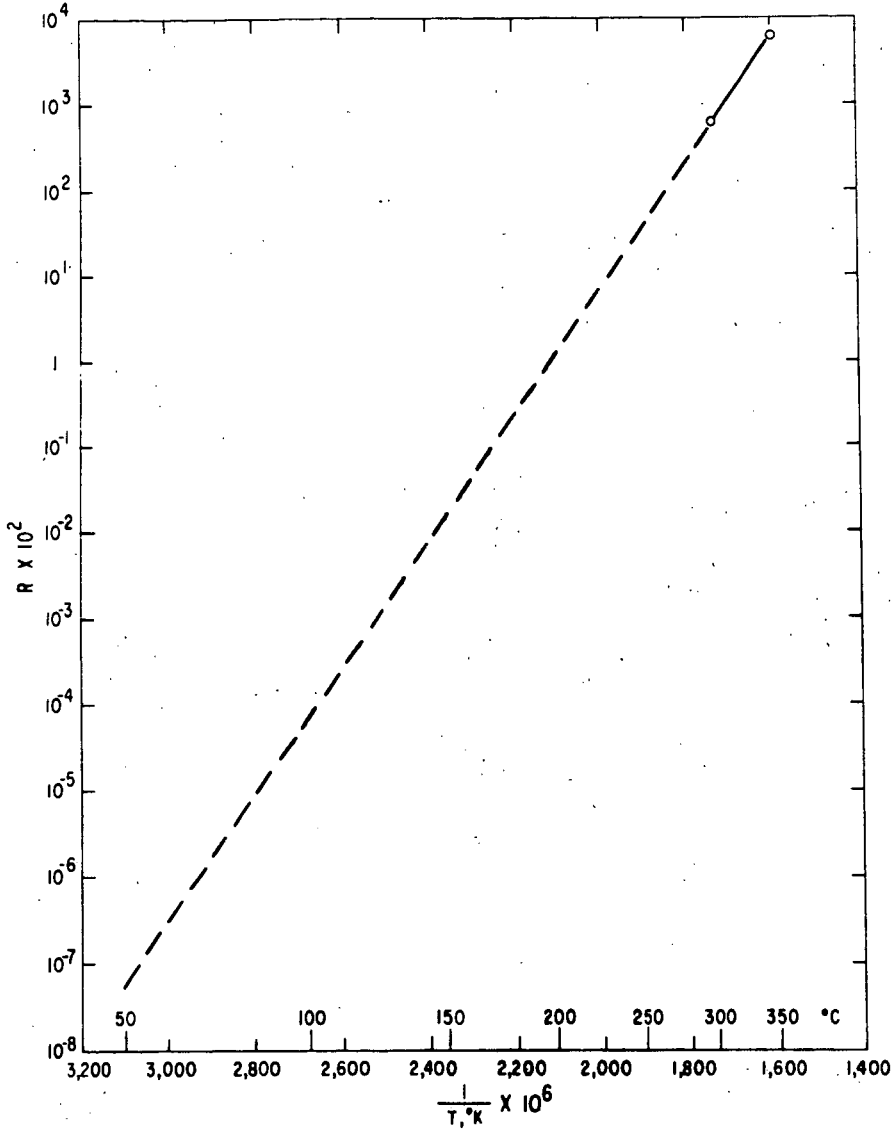


FIGURE 5.- Percent Conversion of Kerogen to Pyrolytic Products in One Year at Various Temperatures.